Norwegian School of Economics
Bergen, Fall 2023

Beyond the Gale: Parametric Insurance Pricing for Offshore Wind

Applications of Hierarchical Bayesian Methods, Markov Chain Monte Carlo and Copula-Based Risk Assessment on Zero Generation Events

Simen Stølsnes & Theodor Hellesøy

Supervisor: Geir Drage Berentsen

Master thesis, Economics and Business Administration

Major: Business Analytics

NORWEGIAN SCHOOL OF ECONOMICS

Acknowledgements

We thank our supervisor Geir Drage Berentsen for his valuable insights, recommendations, and enthusiasm throughout the research period. Our appreciation also goes to our co-supervisor Ida Marie Solbrekke for her initial guidance on the research topic, and to Sondre Hølleland for his assistance in data extraction and structuring. Lastly, we thank our friends and family for their support, attention, and advice while writing this thesis.

Norwegian School of Economics

Bergen, December 2023

Simen Stølsnes

Theodor Hellesøy

Abstract

This thesis introduces an innovative pricing model for parametric insurance of zero-generation events at offshore wind farms, mainly focusing on the Norwegian shelf. The model employs a Hierarchical Bayesian approach to analyze the variability of these events, leveraging historical data. The research uses Markov Chain Monte Carlo simulations to estimate posterior Gumbel distributions for zero generation events on both monthly and regional scales. A significant aspect of the study involves using copulas to model co-dependency between wind farms within a portfolio, and employing Value-at-Risk and Expected Shortfall metrics for risk assessment.

A crucial finding is the heightened risk in insuring portfolios of geographically proximate wind farms due to co-dependency, evident in increased premiums and risk metrics. Additionally, the thesis explores the impact of co-dependency on insurance premiums, noting a trend reversal in premiums based on a trigger event threshold. The research concludes that insurance companies can effectively utilize this pricing strategy for insuring multiple wind farm locations, encouraging offshore wind sector investment by securing operator revenue streams.

Keywords – Offshore Wind, Parametric Insurance, Hierarchical Bayesian Modelling, Markov Chain Monte Carlo Simulation, Copula, Value-at-Risk, Expected Shortfall

Contents

List of Figures

List of Tables

1 Introduction

1.1 Context & Background

In recent years, European nations have significantly advanced their offshore wind energy initiatives, amassing 32 GW capacity by mid-2023 (O'Sullivan, 2023). In August 2023, Equinor launched Hywind Tampen on the Norwegian shelf, serving as the world's first offshore wind farm dedicated to powering oil and gas fields (Equinor, 2023). With an 88 MW capacity, this project aims to reduce CO2 emissions by supplying renewable energy to the Gullfaks and Snorre platforms. This initiative aligns with Norway's environmental strategy, as highlighted in the "Grønt Industriløft" report, which emphasizes the country's commitment to leading in renewable energy development (Regjeringen, 2022). Identifying offshore wind as pivotal to realizing this vision, the Norwegian government unveiled a strategy to allocate zones for up to 30 GW of offshore wind energy by 2040 (Statsministerens kontor, 2022). As of 2023, Norway has announced competition for two offshore wind project areas, Utsira Nord and Sørlige Nordsjø II, with a focus on generating renewable energy to power not only offshore operations but also the mainland (Regjeringen, 2023). Further expansion is planned, with three additional areas expected to open for competition in 2025 (Olje-og energidepartementet, 2023). This strategic pivot towards sustainable energy aligns with the global commitment set forth by the 2015 Paris Agreement, which aims to limit global warming to below 2 degrees Celsius and, ideally, under 1.5 degrees Celsius (FN, 2023).

Despite good conditions for wind production at the Norwegian shelf, wind speeds in this area are highly variable (Solbrekke and Sorteberg, 2022b). This variability causes a risk for owners and operators of the plants due to the inherent uncertainty related to wind. Investments in offshore wind farms are expensive endeavors. Unpredictable wind power generation will directly affect the return rate of investments. Thus, predictable revenue streams are essential for maintaining operations and making offshore wind farms a desirable investment area. Ensuring predictable revenue streams is especially important if the ambitious 30 GW goal is deemed realistic. A way of creating revenue streams from offshore wind farms that are more foreseeable is through parametric insurance, where payouts are triggered by predefined events and the payout amount is predetermined. In

this thesis, we propose a pricing model for a parametric insurance product that pays the customer when there are halts in electricity production at offshore wind farms. Our model is tailored towards future owners and operators of wind farms on the Norwegian shelf. It can, however, be generalized to other areas if the need arises.

1.2 Review of Current Literature

Parametric insurance, a product offering predetermined payouts based on specific triggers, is increasingly relevant in covering risks, notably in wind farms (Beate Drewing and François Lanavère, 2021). This insurance model boasts operational efficiency, primarily due to its streamlined claims process and reduced underwriting costs. Operational efficiency in this insurance model arises from objective events triggering payouts. The need for manual claim inspections and lessening adverse selection issues are therefore diminished (Lin and Kwon, 2020). Furthermore, Lin and Kwon (2020) highlights the model's inherent 'basis risks,' categorized into positive and negative types. Positive basis risk occurs when payouts exceed actual losses, potentially increasing the insurer's insolvency risk. Negative basis risk involves payouts that inadequately cover losses, risking customer dissatisfaction. These risks necessitate careful calibration and ongoing adjustment of parametric triggers to balance insurer and insured interests equitably.

Parametric insurance's flexibility is demonstrated in its application to agriculture and nature-related risks. For instance, Nyagadza et al. (2019) devise a parametric framework for disaster risks in Zimbabwe, and Bhaumik (2008) develops a rainfall-based crop insurance model in India. Additionally, earthquake risk management has seen parametric model innovations, with Pai et al. (2022) employing Bayesian methods for a pricing model in China and Radu and Alexandru (2022) proposing a similar model for Romania. These diverse applications highlight parametric insurance's adaptability across various contexts and geographical areas.

This thesis employs a Bayesian approach to discern patterns in wind power generation, leveraging statistical methods that systematically incorporate prior knowledge, weigh experimental data, and model experimental error (Lu et al., 2002). Bayesian methodologies are widely used to analyze variables with pre-existing knowledge (Shiffrin et al., 2008; Ciucci and Chen, 2015; Palmer et al., 2017; Song et al., 2020; Xiao et al., 2021; Bozorgzadeh

and Bathurst, 2022). Hierarchical Bayesian Models and their application in time series are detailed in Good (1980) and Berliner (1996), respectively. Brooks (1998) review the Markov Chain Monte Carlo (MCMC) method, contributing to the Handbook of Markov Chain Monte Carlo (Brooks et al., 2011). Hamiltonian Monte Carlo is introduced conceptually by Betancourt (2018), and the No U-Turn Sampler's (NUTS) efficacy in genetic parameter evaluation is examined by Nishio and Arakawa (2019). Software packages for HBMs in R and Python, like *brms* and *PyMC*, facilitate intuitive modeling and hierarchy incorporation (Bürkner, 2017, 2018; Patil et al., 2010). Wilkie and Galasso (2022) propose an HBM for UK offshore wind farm capacity factors, providing inspiration for this research.

Understanding production halt risks in multiple wind farms at the time involves modeling their co-dependence, for which copulas are employed. Coined by Sklar (1959), copulas model variable co-dependencies based on marginal distributions, crucial in financial risk management (Embrechts et al., 2003). Energy sector copula applications include analyzing German wind farm spatial dependency (Grothe and Schnieders, 2011), vine copula-based wind power output dependency analysis (Qiu et al., 2019), wind speed correlation uncertainty modeling (Sun et al., 2016), and stochastic wind power correlations using Monte Carlo techniques and pair-copulas (Wang et al., 2016). Relevant to this study are master's theses from the Norwegian School of Economics that explore copula modeling of spatial dependence in offshore wind farms along the Norwegian shelf (Alfsvåg and Sollie, 2023; Wallevik and Klock, 2022).

Research on insurance strategies to mitigate wind power uncertainty includes Monte Carlo simulations for estimating insurance premiums (Yang et al., 2016) and creating insurance products for power imbalance risks (D'Amico et al., 2017). Thakur et al. (2023) suggests binary option contracts for short-term revenue risk hedging in wind farms. Han et al. (2019) propose a weather-indexed pricing model using yearly contracts, leveraging wind speed and generation data to form a wind-power index. Payouts are triggered when this index surpasses a certain threshold, helping reduce economic losses for wind power producers.

1.3 Research Question

Despite existing research on indexed-based insurance models in wind power, parametric insurance pricing models specifically addressing production halts in offshore wind farms remain under-explored. Moreover, the co-dependence of production halts across different wind farm locations has to the best of our knowledge not been studied. In light of substantial investments in offshore wind production on the Norwegian shelf, this research gap becomes significant. Our study aims to enhance the security and predictability of operations and investments in this sector by developing a robust pricing model for a parametric insurance product. Drawing inspiration from Wilkie and Galasso (2022), we estimate the monthly percentage of zero generation events (ZG) at Norwegian offshore wind farms using a Hierarchical Bayesian approach with Markov Chain Monte Carlo simulations, specifically the No U-Turn Sampler algorithm. Additionally, the research will assess how insuring portfolios of wind farms affects the insurer's risk profile and pricing strategies with the use of copulas.

How can pricing be optimally structured for parametric insurance that caters to individual offshore wind farms, and what are the implications of elevated risks when managing multiple wind farm operations? Furthermore, how does the trigger event threshold value influence the overall insurance premium? These considerations form the foundation for our central research question:

In what ways can insurers effectively price parametric insurance products for offshore wind farms, considering the ZG co-dependency risks between wind farm locations?

2 Data

In this section, the data used for our analysis is showcased. The section also offers an overview of the data through descriptive statistics and figures. The general inspections in this section form the foundation of our Bayesian and Copula approaches.

2.1 NORA3-WP

The data analyzed is extracted from the source called NORA3-WP. This high-resolution wind power and wind resource dataset covers the North Sea, the Baltic Sea and parts of the Norwegian and Barents Sea (Solbrekke and Sorteberg, 2022a). The data is presented on a monthly basis, and the variables are stored on a 3x3 km horizontal grid covering the relevant areas. Data is collected from 1996 to 2019. Solbrekke and Sorteberg (2022a) states that the data is created for "research and usage in the planning phase of new wind farms", making it suitable for our thesis.

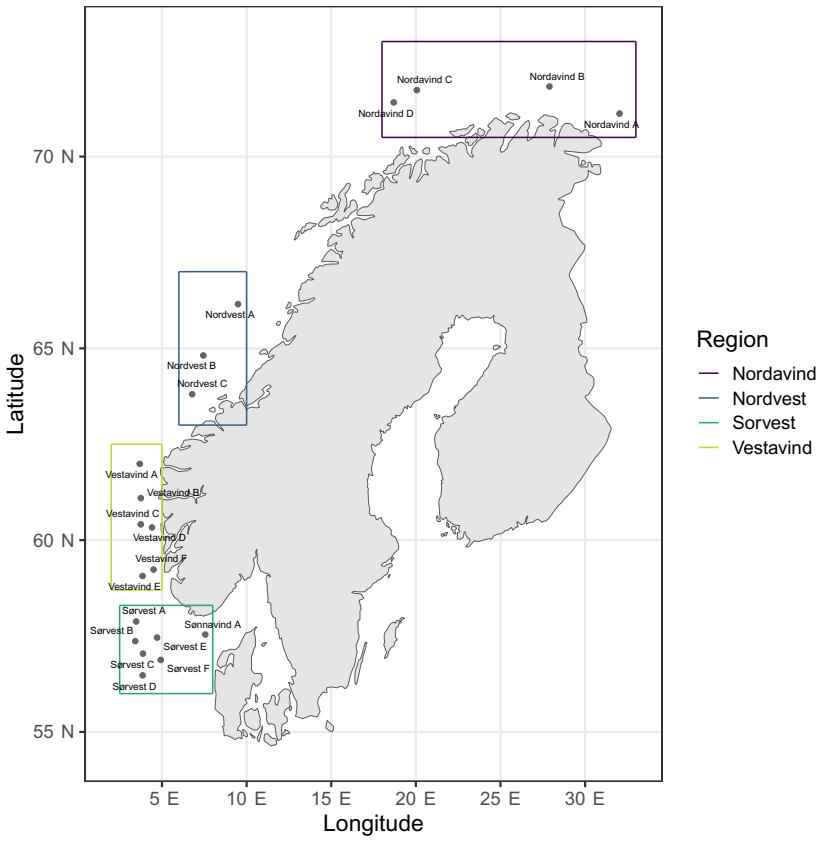

Figure 2.1: Locations and regions

The data in the analysis is limited by focusing on representative grid points from 20 distinct locations. These locations have been selected based on their suitability for offshore wind projects on the Norwegian shelf, as recommended by the Norwegian Water Resources and Energy Directorate (NVE, 2023). A visual representation of these sites along the Norwegian coastline is presented in figure 2.1. For clarity, these sites have been categorized into four primary regions: *Nordavind*, *Nordvest*, *Vestavind*, and *Sørvest*. Location Sønnavind A is incorporated within the Sørvest region due to its geographical proximity.

Wind power variables in the data are derived using three distinct wind turbines: Siemens' SWT-6.0–154, and the reference turbines DTU-10.0-RWT and IEA-15–240-RWT. Each of these turbines possesses different technical specifications. As illustrated in figure 2.2, there are subtle variations in their cut-in values. However, the outcomes of the analysis are anticipated to remain consistent regardless of the turbine selected. For the purpose of this thesis, the focus will be exclusively on the IEA-15–240-RWT reference turbine.

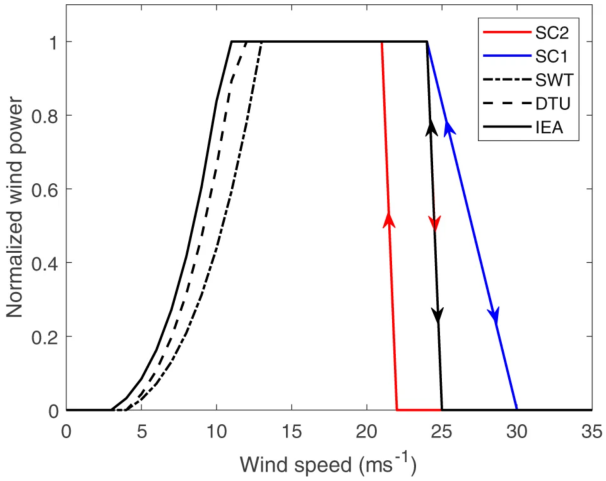

Figure 2.2: Power curves (Solbrekke and Sorteberg, 2022a)

The primary variable under examination is termed *zero_generation* (ZG). This metric denotes the monthly proportion of zero generation events at a specific grid point. ZG occurs, either due to wind speeds that are too low, or excessively high. The cut-in value represents the lower threshold, while the cut-off value signifies the upper limit. The power curves for all turbines are depicted in figure 2.2. For the turbine central to our analysis, the cut-in value stands at 3 m/s, and the cut-off value is set at 25 m/s. Wind speeds outside this range result in ZG.

2.2 Descriptive Statistics

ZG and how it occurs across different locations is central for this thesis. Figure 2.3 shows the average number of times ZG at a specific location exceeds 10.08 % (75th percentile) ZG annually. There are geographical differences by inspecting the return periods of ZG. Locations in region Sørvest have lower return periods, while locations in regions Vestavind and Nordvest have notably higher return periods.

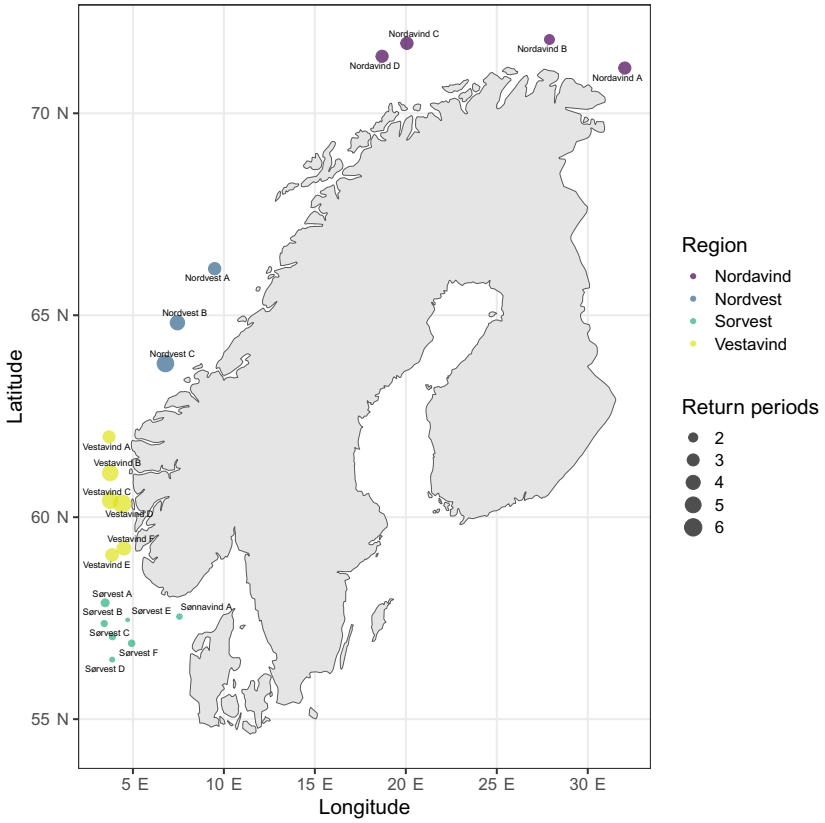

Figure 2.3: Return periods of ZG above 75th percentile

The average ZG across months for the locations is visualized in figure 2.4. The figure displays seasonal patterns in the data. ZG occurs more often in the summer months than in the winter months. Also, variations of ZG across the locations are seen. Sites within the Sørvest region have lower values of ZG, while sites in the Vestavind region have higher values of ZG, as suggested by studying figure 2.3.

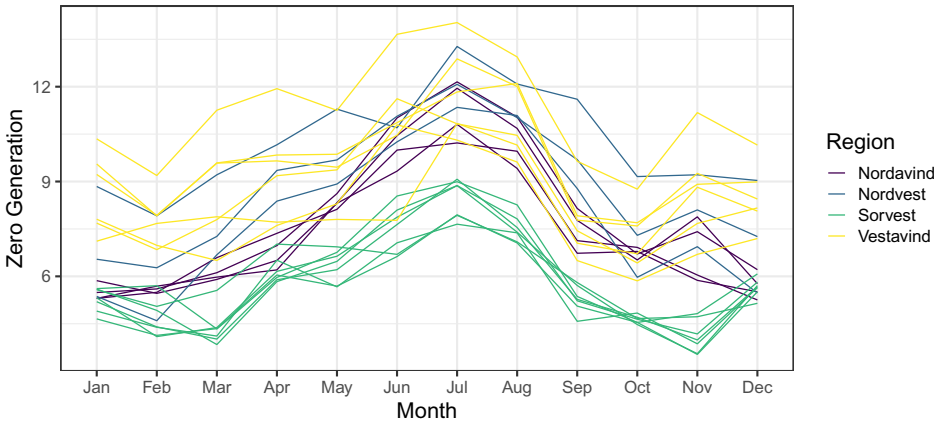

Figure 2.4: Average zero generation by months.

The data for each location is limited. Spanning from 1996 to 2019, each specific month at a given location comprises only 24 data points. However, data at the regional resolution will result in more data observations. Figure 2.5a illustrates the correlations of ZG across all locations. Upon examining this figure, it becomes evident that locations within a shared region exhibit the strongest correlations. Exceptions to this observation are seen in specific Vestavind locations, which appear to have a pronounced correlation with some sites in Sørvest. The geographical proximity of these locations can explain this correlation. Figure 2.5b underscores the trend that closer locations generally manifest higher correlations. The color gradations in this plot further emphasize that locations within the same region tend to be the most correlated. These regional demarcations are further used for analysis to ensure sufficient sample sizes.

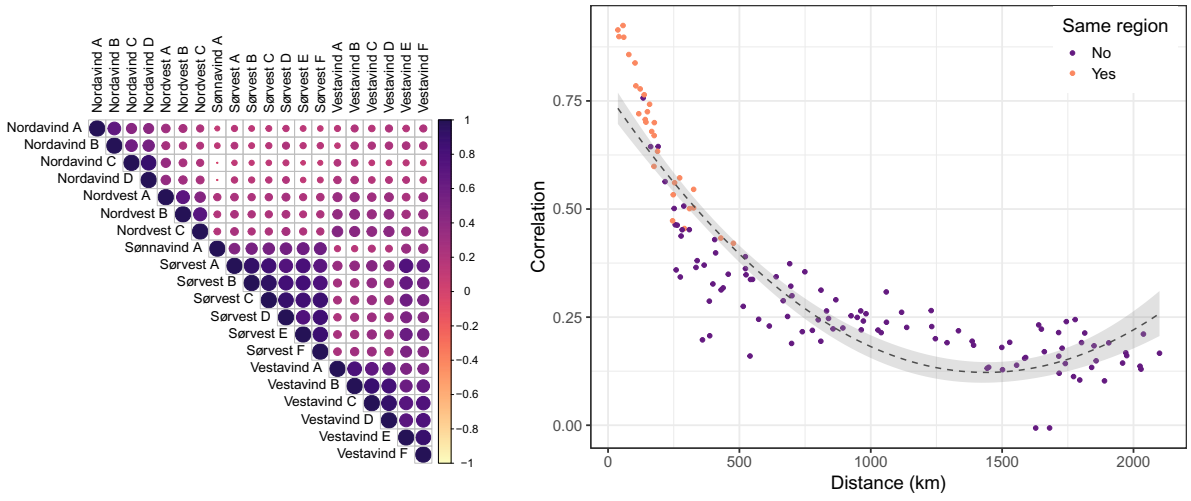

(a) Correlation

(b) Correlation vs distance

Figure 2.5: Correlation plot and distance vs correlation plot.

Figure 2.6 presents histograms illustrating the distribution of ZG across regions. The number of data points in each region differs due to the varying number of locations within the region. Despite this variation, the shape of the regional distributions resembles each other across all regions. The data points range from a minimum of 0 to a peak slightly above 30%. This maximum value is observed in the Vestavind region.

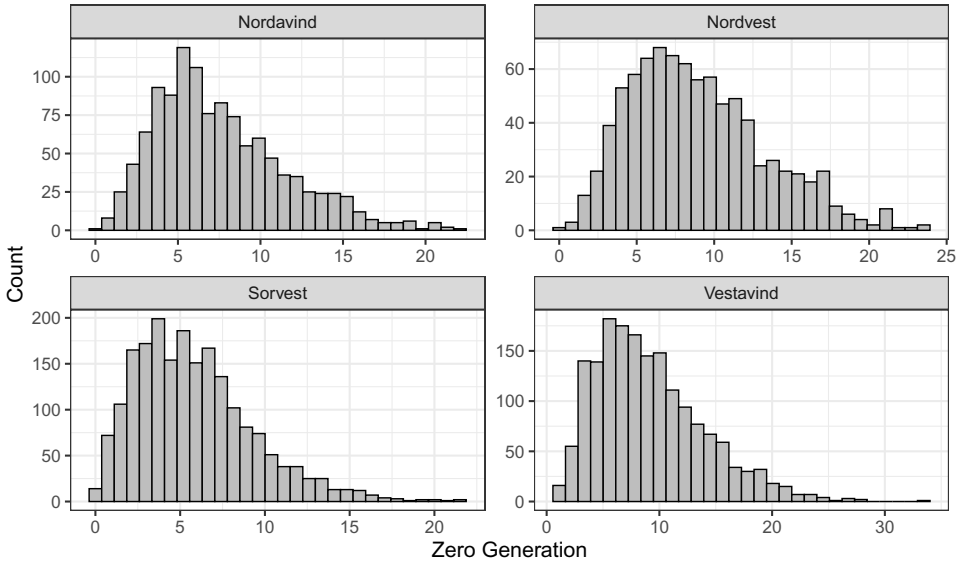

Figure 2.6: Histograms of regions

A distinct feature of the data is its pronounced right tail. From an insurer's perspective, the frequency of payouts varies based on the likelihood of surpassing a threshold of ZG. Underestimation of the right tail could expose the insurer to considerable financial risks, as it may lead to a higher volume of claims than anticipated. Conversely, for the insured party, a long tail signifies the presence of outlier values that could lead to substantial losses. For a parametric insurance product to be viable and appealing, the total payouts must cover a significant portion of the losses incurred. These considerations necessitate adopting a model that effectively captures the tail behavior. Section 3.1.3 further elaborates and discusses this topic

3 Methodology

This section introduces the necessary concepts and definitions for understanding the methodology used in this thesis. It elaborates on the methods used to estimate marginal probability distributions of ZG for wind farms. Secondly, it presents the estimation of joint probability distributions of ZG in combinations of wind farms. Lastly, it elaborates upon the practical use of these methods for creating a parametric insurance pricing model.

3.1 Model Definition

A Hierarchical Bayesian Model (HBM) utilizes statistical principles presented and formulated by the Reverend Thomas Bayes. HBMs use prior knowledge to influence the model's beliefs about a specific event's probability. The models are hierarchical, meaning prior beliefs about explanatory factors influence our posterior probability distribution hierarchically. Posterior probability distributions refer to the estimated probability distribution that best fits our data after our prior probability distributions have influenced our beliefs (Lee, 2023). A hierarchical approach is chosen to model regional variability in ZG and combined regional-monthly variability in ZG. Section 3.1.1 explains this further.

3.1.1 Prior- & Posterior Definition

Our study models X_{it}, representing ZG for region i during month t. Posterior probability distributions are estimated on the region level to account for sparse data on the location level, as discussed in section 2.2. Estimated distributions for a given region i are thereby assumed to represent the underlying distributions of ZG at a specific location within its region. Figure 3.1 visually represents the HBM framework used in this study.

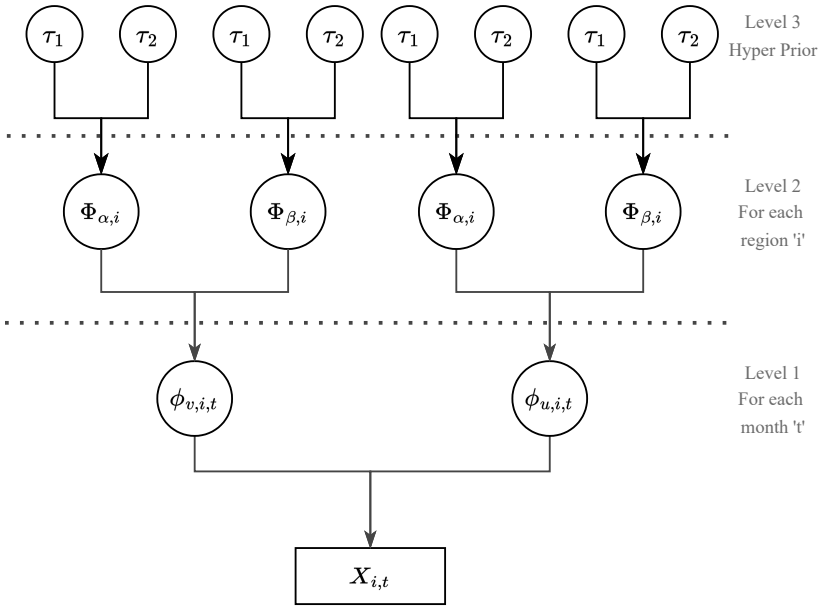

Figure 3.1: Graphical representation of the HBM

Four posterior distributions of differing families are estimated using different likelihood functions, as elaborated upon in section 3.1.3. ϕ_{uit} and ϕ_{vit} denotes the parameters for the likelihood function. These adhere to Level 1 of the hierarchy and represent the parameters of region-month-specific marginal posterior distributions. The index i represents a given region out of I regions, and t represents a given month out of T months. The region-month-specific parameters account for monthly variation influenced by a common underlying factor specific to each region. Region-month-specific parameters are drawn from Gamma priors in Level 2 of the hierarchy. The parameters at Level 2 are region-specific and only contain information about the regional variability in X_{it}. Level 2 parameters represent the shape $\Phi_{\alpha i}$ and rate $\Phi_{\beta i}$ parameters, of which region-month specific parameters ϕ_{vit} and ϕ_{uit} are drawn. The hierarchy's structure implies that Level 1 region-month-specific parameters share information about a region at Level 2. Thus, if differences exist in the seasonal pattern of X_{it} between regions, the model's ability to estimate region-month-specific parameters allows it to discern and reflect these variations. Level 2 parameters are drawn from Gamma distributions with parameters from Level 3 of the hierarchy. Level 3 comprises hyper-priors drawn from a $\Gamma(2, 1)$ distribution. The hyper-priors τ_1 and τ_2 represent shape and rate parameters for the distribution of the region-specific parameters $\Phi_{\alpha i}$ and $\Phi_{\beta i}$.

The choices of prior distributions account for three primary factors that defined our prior beliefs about X_{it}. Firstly, the distribution of X_{it} is right-skewed and rarely observed as strictly 0. Secondly, the region in question explains some of the variability of X_{it} due to the geographical diversity between regions. Finally, the month in question explains some of the variability of X_{it} due to the seasonal component visualized in figure 2.4. The resulting joint posterior distribution of the parameters, given observed data, is defined by the following expression:

$$p(\phi_{vit}, \phi_{uit}, \Phi_{\alpha i}, \Phi_{\beta i}, \tau_1, \tau_2 | X_{it}) \propto p(\tau_1)p(\tau_2) \prod_{i=1}^{I} p(\Phi_{\alpha i}|\tau_1, \tau_2)p(\Phi_{\beta i}|\tau_1, \tau_2) \times \prod_{i=1}^{I}\prod_{t=1}^{T} p(\phi_{vit}|\Phi_{\alpha i}, \Phi_{\beta i})p(\phi_{uit}|\Phi_{\alpha i}, \Phi_{\beta i})p(X_{it}|\phi_{vit}, \phi_{uit}) \tag{3.1}$$

The letter p represents probability distributions. All parameter estimations condition on data corresponding to the given indexes. I.e, ϕ_{vit} for $i = \textit{Nordvaind}$ and $t = 3$ is estimated given the data indexed with the same i and t. Each set of parameter estimates is calculated twice because the HBM employs 2-parameter distribution families. For Level 1, there are $2 \times I \times T$ parameter estimates, while Level 2 has $2 \times I$ parameter estimates. Level 3 contributes two parameter estimates, reflecting the hyper-priors. Given that $I = 4$ and $T = 12$, this amounts to 106 parameter estimates for each posterior distribution.

The joint posterior distribution of the parameters in equation 3.1 is proportional to the product of the prior distributions of the hyperparameters and the parameters and the likelihood of the observed data. This proportional relationship is a fundamental tenet of Bayesian inference, where the posterior distribution combines prior beliefs with the likelihood of the observed data. The priors represent our initial understanding of the parameter distributions, updated upon observing the data X_{it}. The likelihood term $p(X_{it}|\phi_{vit}, \phi_{uit})$ incorporates the observed data into the inference process, ensuring that the posterior distribution informs the data and the priors (Lee, 2023). The HBM is formulated in Python code, and distributional parameters are estimated using the PyMC-package (Patil et al., 2010). After estimating region-month specific parameters ϕ_{vit} and ϕ_{uit}, marginal posterior distributions for X_{it} are defined as follows:

$$X_{it} \sim f(X_{it}|\phi_{vit}, \phi_{uit}) \quad \forall\ i \in I,\ t \in T \tag{3.2}$$

3.1.2 Markov Chain Monte Carlo Simulation

Markov Chain Monte Carlo (MCMC) simulation is an essential tool for parameter estimation within a HBM framework. MCMC integrates the independent sampling power of Monte Carlo simulations with the convergence properties of Markov Chains. This attribute is fundamental in Bayesian estimation due to the complex dependency structures inherent in such models. Consequently, MCMC is a robust method for estimating both prior and posterior parameters, ensuring that the Bayesian inferences drawn are reliable and accurate (Lee, 2023).

"Monte Carlo simulation is the process of generating random values for uncertain inputs in a model, computing the output variable of interest, and repeating this process for many trials to obtain a distribution of the output" (Laguna and Marklund, 2019, p. 262). Further, Ordinary Monte Carlo simulation is referred to as OMC. Markov chains are defined as a sequence $X_1, X_2, ...$ of random elements where the conditional distribution of X_{n+1} given $X_1, ..., X_n$ depends on X_n only. "A Markov Chain has *stationary transition probabilities* if the conditional distribution of X_{n+1} given X_n does not depend on n. This Markov Chain is the one of interest in Markov Chain Monte Carlo" (Brooks et al., 2011, p. 4). A Markov chain has *converged* if it reaches its stationary distribution.

Furthermore, "the theory of MCMC is just like the theory of OMC, except that stochastic dependence in the Markov chain changes the standard error" (Brooks et al., 2011, p. 8). " Hamiltonian Monte Carlo (HMC) is an increasingly popular alternative MCMC method. HMC adopts Hamiltonian dynamics in physics to propose future states in the Markov chain". This method, however, relies heavily on the choice of two hyperparameters. The No U-Turn Sampler (NUTS) is an HMC. "NUTS uses a recursive algorithm to automatically tune the HMC algorithm without requiring user intervention or costly tuning runs" (Nishio and Arakawa, 2019, p. 2). NUTS is packaged into multiple sources of software like Stan, the BGLIMM procedure in SAS, and the PyMC package for Python (Patil et al., 2010). For this thesis, the PyMC-package (version 5.9.0) is used to perform MCMC estimations of the marginal posterior probability distributions $\hat{f}(X_{it})$ for all regions, i, and months, t.

The *pymc.model*-function and the *pymc.sample*-function are used to generate samples for the HBM. The model runs with four independent chains, a decision that aids in assessing

the convergence and reliability of the sampling process; convergence of all chains to a similar distribution indicates correct sampling from the posterior. Convergence diagnostics are further explained in section 3.1.4. The function draws a given amount of samples from the posterior distribution, including a pre-determined amount of tuning iterations. The tuning samples are discarded when computing summary statistics, as they do not represent the desired distribution. Additionally, a target acceptance rate of 0.80 is specified for the NUTS algorithm. This target acceptance rate reflects a balance between the step size of the sampler and the rate at which proposed samples are accepted, enhancing the efficiency of the sampling process.

3.1.3 Distributional Families

As stated in section 2.2, our data exhibits a degree of right-skew and long-tail behavior. Given these considerations, the Beta, Inverse Gamma, Weibull, and Gumbel distributions emerged as potential candidates for marginal posterior probability distributions. The Gumbel distribution, unlike the other families, can yield negative values. Intuitively, this may seem incongruous when estimating shares of ZG. However, for the thesis, this characteristic is not detrimental. The primary focus is estimating probabilities that ZG will exceed a specified positive threshold. Thus, the potential for negative values does not impact the accuracy or relevance of the pricing model if it can effectively explain the underlying data's probability distribution. The Gumbel family is therefore included when comparing distributional families in the next section (3.1.4).

We employed the PyMC library (Patil et al., 2010) to estimate the posterior distributions, applying the definition outlined in equation 3.1. This process is repeated for each of the four distributional families under consideration. We adapted the likelihood function within our model for each family to correspond with the specific distributional family evaluated.

3.1.4 Model Comparison

When estimating posterior probability distributions, it is crucial to explore different candidates and compare their performance against each other. Watanabe–Akaike Information Criterion (WAIC) (Watanabe and Opper, 2010), and Pareto Smoothed

Importance Sampling Leave-One-Out Cross-Validation (PSIS-LOO) (Vehtari et al., 2017) are two different measurements used for such purposes. These measurements aim to balance goodness-of-fit to the data and complexity. Vehtari et al. (2017) uses a measure of predictive accuracy, Expected Log Pointwise Predictive Density (ELPD), to maintain comparability between the two measurements.

Four different HBMs with differing distributional families are estimated, as stated in section 3.1.3. MCMC simulations are run for 1000 tuning iterations and 2000 sampling iterations with 4 Markov chains. Comparison measurements, *ELPD LOO* and *ELPD WAIC*, are calculated for each HBM and used for model comparison. The model with the highest values of *ELPD LOO* and *ELPD WAIC* is chosen and estimated by MCMC simulation with 2500 tuning iterations and 10000 sampling iterations to ensure proper sample sizes and convergence of the Markov chains.

Convergence of Markov chains when executing MCMC is essential. Estimates from any MC simulation are only valid if the Markov chains have converged. Markov chain convergence is evaluated through visual inspection of a plot of the chain's trace (also called a traceplot). According to Peng (2022b), the theory claims that all Markov chains run in an MCMC simulation should eventually converge to the stationary distribution. Convergence can be visually confirmed when the traceplots are noisy and exempt from clear patterns. Convergence is also evaluated by calculating the Gelman-Rubin diagnostic (Peng, 2022a). If $\hat{r}$ is approximately equal to 1, the chain has converged. Increasingly high values of $\hat{r}$ indicates divergence in the Markov chain of interest.

3.2 Pricing Model for a Single Wind-Farm

Calculating the premium of a pricing model with monthly-based contracts considers the probability of a certain amount of ZG during a given month t, at a given region i, exceeding a threshold denoted as k.

3.2.1 Monthly Contracts

Parametric insurance pays a pre-defined amount to the customer whenever a trigger event occurs. This payout is referred to as L. The price of a monthly contract of parametric

insurance for a single offshore wind farm in region i during month t is defined as follows:

$$premium_{it} = E(1_{\{X_{it}>k\}}) \cdot L = P_{\hat{f_{it}}}(X_{it} > k) \cdot L \tag{3.3}$$

If X_{it} exceeds the threshold k with a probability defined by an estimated marginal posterior distribution $\hat{f}_{it}$ at a wind farm in the region i during a given month t, an amount equal to L is paid out to the customer by the insurer.

3.2.2 Yearly Contracts

This thesis assumes independence between months for all types of yearly contracts. Thus, the price of a yearly contract of parametric insurance for a single offshore wind farm in the region i is defined as the monthly contract, summed over the next T months after purchasing the insurance product. $T = 12$ for all calculations of yearly contracts:

$$premium_i = \sum_{t=1}^{T} E(1_{\{X_{it}>k\}}) \cdot L = \sum_{t=1}^{T} P_{\hat{f_{it}}}(X_{it} > k) \cdot L \tag{3.4}$$

3.3 Pricing Model for a Portfolio of Wind-Farms

The positive correlation of ZG events across geographically similar wind farms, as illustrated in figure 2.5a, underscores the necessity for modeling co-dependency between wind farm locations within a portfolio. This approach is vital for accurately assessing and managing the elevated risks associated with insurance policies for offshore wind farms. By modeling co-dependency, insurers can more effectively evaluate potential losses due to simultaneous ZG events in a portfolio of wind farms, leading to more robust and tailored risk management strategies. The development of a pricing model for a portfolio of wind farms is motivated by this, aiming to accurately reflect the interconnected risk factors and optimize insurance premium strategies.

Until now, the variable X_{it} has represented the occurrence of ZG in a given region, denoted by the index i, during month t. However, as we shift our focus towards the pricing model for insurance policies covering portfolios of wind farms, the variable X_{nt} is introduced. The index n represents an individual wind farm location within a portfolio of N wind farms.

X_{nt} is assumed to follow the corresponding region-month-specific posterior distribution defined in equation 3.2. $f(X_{nt})$ is defined as the marginal probability distribution of ZG at location n and month t.

$$f(X_{nt}) = f(X_{it}|\phi_{vit}, \phi_{uit}) \quad \forall\ n \in i \tag{3.5}$$

where n represents one of N wind-farm locations in a chosen portfolio located in region i. The likelihood that the sum of ZG in the portfolio exceeds a specified threshold k determines the pricing for a portfolio of wind farms. Again, independence between months is assumed. Yearly contracts are calculated using models for each month in the same way as the case for insurance of a single wind farm defined in section 3.2.2. For a given month t, the sum of ZG in a portfolio is defined as:

$$Y_t = \sum_{n=1}^{N} X_{nt} \tag{3.6}$$

All examples of portfolios in this thesis contain $N = 3$ wind farms. This simplification is done for comparison purposes. The pricing model can be used on any number of wind farms in a portfolio.

3.3.1 Copula Distributions

Multivariate copulas are fit to capture the co-dependence between ZG at wind farms in a portfolio effectively. Copulas are mathematical constructs that capture the dependence structure between random variables, independent of their individual marginal distributions. Essentially, they present the correlation or dependency patterns among several variables without being tied to the specific form of their individual distributions. Copulas can model the joint behavior of ZG, ensuring risk assessments factor in the nuances of mutual interactions. According to Sklar (1959), a copula with continuous marginals exists for any joint distribution. Hence, the copula representing the joint distribution for any pair of months and location can be defined as follows:

$$F(X_{1t}, ..., X_{Nt}) = C(F_1(X_{1t}), ..., F_I(X_{Nt})) \tag{3.7}$$

where $F(X_{nt})$ is the cumulative distribution function (CDF) for each combination of wind farm location n and month t in the portfolio. The transformed observed values using the CDF should be uniformly distributed on the interval $[0, 1]$. Copulas of different families are estimated and compared using the *copula*-package in R. Specifically, the *fitCopula*- and *gofCopula*-functions are used (Hofert et al., a,b).

3.3.2 Copula Family Comparison

The goodness-of-fit tests are based on the process of comparing the empirical copula with a parametric estimate of the copula derived under the following null hypothesis:

$$H_0 : C \in C_0 \tag{3.8}$$

The null hypothesis states that "the dependence structure of a multivariate distribution is well represented by a specific parametric family of copulas" (Genest et al., 2009). Cramér-von Mises test statistics (hereby referred to as CMT) and p-values are calculated. Large values of CMT reject the null hypothesis. Conversely, p-values under approximately 5% reject the null hypothesis.

3.3.3 Yearly Contracts for a Portfolio of Wind Farms

The distribution of a portfolio's joint variability of ZG is estimated using OMC simulation. The first step is to fit a copula for a portfolio with N locations in month t: $\hat{C}_t(F_1(X_{1t}), ..., F_N(X_{Nt}))$. Copulas are fit using the marginal distribution for each location in the portfolio, $f(X_{nt})$. Uniform values on the interval $[0, 1]$ are obtained using the corresponding cumulative distribution function, $F(X_{nt})$. These uniform values are input for the *fitCopula()*-function, which utilizes Maximum Pseudo-Likelihood to estimate multivariate distributions for a given portfolio (Hofert et al., a).

After fitting the copula, R samples are drawn from $\hat{C}_t$. The sample draws are defined as $(X_{1tr}, ..., X_{Ntr})$, where the index $r \in R$ denotes the iteration of the OMC simulation. Drawn values are expressed as uniform values. The quantile function corresponding to the distribution $f(X_{nt})$ is used to return the $R \cdot N$ uniform values to their original scale. This function is tailored to the unique marginal distribution of each location n in the portfolio. This process results in R estimates of ZG for every location n in the portfolio

during month t. The portfolio sum of each sample estimate is defined as follows:

$$Y_{tr} = \sum_{n=1}^{N} X_{ntr} \quad \forall \quad r \in R,\ t \in T \tag{3.9}$$

The probability of the portfolio exceeding k ZG in month t is then calculated by:

$$\hat{P}(Y_t > k) \approx \frac{1}{R} \sum_{r=1}^{R} 1_{\{\hat{Y}_{tr} > k\}} \quad \forall \quad t \in T \tag{3.10}$$

$\hat{P}(Y_t > k)$ is the MC estimated probability that the portfolio-sum of ZG, Y_t in month t will exceed the threshold k. The price of the insurance contract for one year is therefore defined as:

$$premium = \sum_{t=1}^{T} \hat{P}(Y_t > k) \cdot L \tag{3.11}$$

3.3.4 Value-at-Risk & Expected Shortfall

The measures Value-at-Risk (VaR) and Expected shortfall (ES) are used to evaluate risks of co-dependency within a portfolio of wind farms.

VaR was introduced by J.P.Morgan in the 1990s (J.P.Morgan, 1996). They define VaR as "a measure of the maximum potential change in value of a portfolio of financial instruments with a given probability over a pre-set horizon" (J.P.Morgan, 1996, p. 6). An $x\%$ value at risk of Y means that there is an $x\%$ chance that losses will not exceed Y. However, VaR does not estimate losses occurring for the specific scenarios that exceed the VaR threshold.

ES was introduced by Rockafellar and Uryasev (2000). This metric is linked to Value at Risk (VaR), serving as an extension to measure potential losses. Essentially, ES computes the average of all losses that surpass the designated VaR threshold. Calculating ES necessitates an initial computation of VaR for a specified threshold. In essence, ES provides an estimation of the expected loss on the occasions where the predefined VaR threshold is exceeded.

Traditionally, VaR and ES are employed as metrics to quantify financial losses. This thesis

adopts an approach whereby the VaR and ES are computed for the portfolio sum of ZG, denoted as Y_t. This approach is used because the analysis aims to evaluate the direct risk associated with ZG when owning a portfolio of wind farms. Two example portfolios are chosen in order to calculate and compare VaR and ES:

$$diverse\ portfolio \in \{\text{Sørvest A, Nordvest B, Nordavind C}\}$$

$$similar\ portfolio \in \{\text{Sørvest B, Sørvest C, Sørvest E}\}$$

The portfolios are *similar* and *diverse* when considering the correlation in ZG between observations and geographical proximity. As seen in figure 2.5b, locations closer to each other exhibit a larger correlation. These considerations motivates the choice of the two example portfolios with varying correlation and degrees of geographical similarity. To assess the added risk of insuring multiple wind farms due to co-dependency, values of ZG are simulated with two separate approaches: Firstly, under the assumption of independent marginal distributions $\hat{f}_{it}$, for each wind farm i, in the portfolio. Secondly, with the joint distribution derived from fitting a Copula as described above. By calculating VaR & ES for both instances, inferences about the risk of co-dependency are made. 95%-VaR is calculated as the 95th percentile of the draws from the dependent and the independent simulations for a given month t and for both example portfolios. 95%-VaR is equal to the value y in equations 3.12 and 3.13:

$$\hat{P}(Y_t > y) = 0.05 \tag{3.12}$$

$$95\%\ \text{VaR} = y \tag{3.13}$$

ES is the mean of the draws above the 95th percentile for both portfolios and simulation instances.

$$\text{ES} = \frac{1}{M}\sum_{t=1}^{m} Y_t \tag{3.14}$$

where $m \in M$ denotes the observations where $Y_t > 95\%$ VaR. The implied risk associated with insuring a portfolio of wind farms is then evaluated by considering the difference between VaR & ES when modeling co-dependence and VaR & ES without co-dependence.

VaR & ES are essential measures to the insurance company, as they assist in considering the worst possible outcomes of ZG, which would trigger unforeseen and large payouts. If the insurance company is unaware of the potentially elevated risks associated with insuring a portfolio of wind farms, it may inadvertently underestimate the likelihood of payouts. Such a miscalculation can lead to a higher frequency of payouts than initially projected, resulting in financial losses for the insurance company.

3.3.5 Calculation of Monthly & Yearly Premiums for a Portfolio

We define four different scenarios: (1) A *similar* portfolio modelled *with* co-dependence, (2) a *similar* portfolio modelled *without* co-dependence, (3) a *diverse* portfolio modelled *with* co-dependence and (4) a *diverse* portfolio modelled *without* co-dependence. OMC simulations, as described in sections 3.3.3 and 3.3.4, are run for all scenarios. The predefined payouts from the insurer, L, are set to 1 NOK. A threshold of $k = 0.3024$ is chosen. The threshold equals the 75th percentile of ZG (see section 2.2), multiplied by the number of wind farms in our example portfolios, $N = 3$. Thus, monthly premiums for all scenarios are calculated using equation 3.10. The difference in the monthly premiums is calculated for scenarios 1 & 2 and for scenarios 3 & 4 to consider elevated risks of co-dependency. Lastly, yearly premiums are calculated as a function of the threshold k, using equation 3.11.

4 Results & Discussion

4.1 Model comparison

The HBM defined in section 3.1 was run as explained in section 3.1.4. Results of PSIS-LOO and WAIC are presented in table 4.1.

Model	ELPD_WAIC	ELPD_LOO	P_LOO	P_WAIC
Gumbel	**11134.11**	**11133.80**	**84.22**	**83.91**
Weibull	11062.28	11061.75	111.54	111.01
Beta	11058.43	11056.96	131.82	130.36
Inverse Gamma	8818.13	8814.49	205.59	201.95

Table 4.1: PSIS-LOO & WAIC metric

When assessing model fit, a higher ELPD estimate suggests a better performance. Among the models we analyzed, the Gumbel-family posterior model stood out, performing best based on both PSIS-LOO and WAIC evaluations. The terms P_LOO and P_WAIC refer to the effective number of parameters in the models. While more parameters can make a model detailed, it also increases the overfitting chance. The model with a Gumbel-family posterior had the fewest effective parameters, indicating a balance between detail and risk of overfitting.

To further review which models had the best fit, posterior predictive checks were done to evaluate the goodness-of-fit of the models. Andrew Gelman and Jennifer Hill (2007) defines *posterior predictive checks* as "simulating replicated data under the fitted model and then comparing these to the observed data". The Kernel Density Estimate (KDE) plot shown in figure 4.1 offers a visual representation between the true distribution of the data and the distribution resulting from our simulated data using one of the family-specific models. This plot shows how well the models with different distributional families mirror the underlying structures and patterns of the observed data.

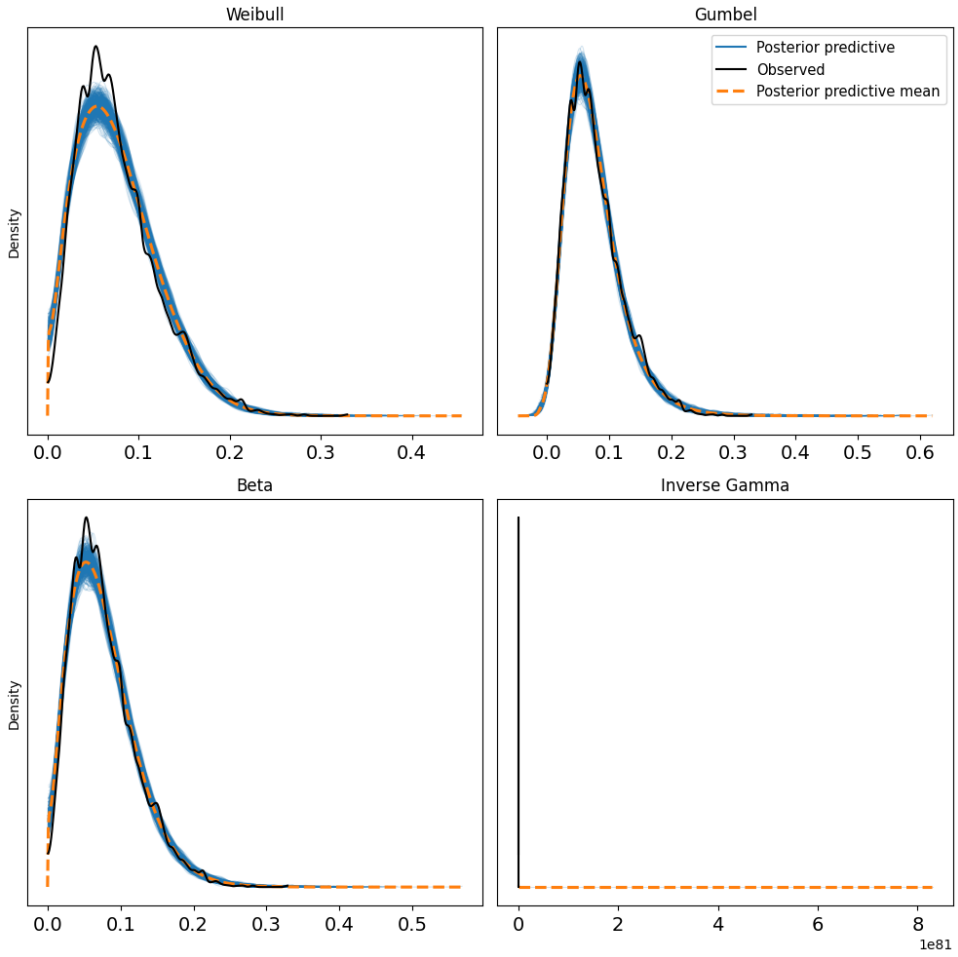

Figure 4.1: Kernel Density Estimate vs. Posterior Predictive Densities & Mean

Examining figure 4.1, it is evident that both the Weibull and Beta models exhibit signs of underfitting at the peak of the distribution. Conversely, in the tails of the distribution, these models tend to overfit. The Inverse Gamma model does not seem to capture the underlying data in any way. In contrast, the Gumbel model aligns more with the observed data. The Gumbel distribution captures the underlying data both in the tails and the peak of the distribution. Therefore, the model with the Gumbel-family posterior shows the best fit for the data compared to the models using alternative distributional families. Given the findings from both posterior predictive checks and our accuracy measurements, the model with the Gumbel-family posterior marginals is chosen to represent the probability of ZG.

4.2 Convergence Diagnostics

An MCMC simulation, as described in section 3.1.4, was run with the Gumbel family posterior. A traceplot for evaluating the convergence of Markov chains is visalized in figure 4.2. A selection of parameter estimations and their summary statistics is presented in table 4.2. All other traceplots and tables of MCMC estimates of distributional parameters are found in the appendix.

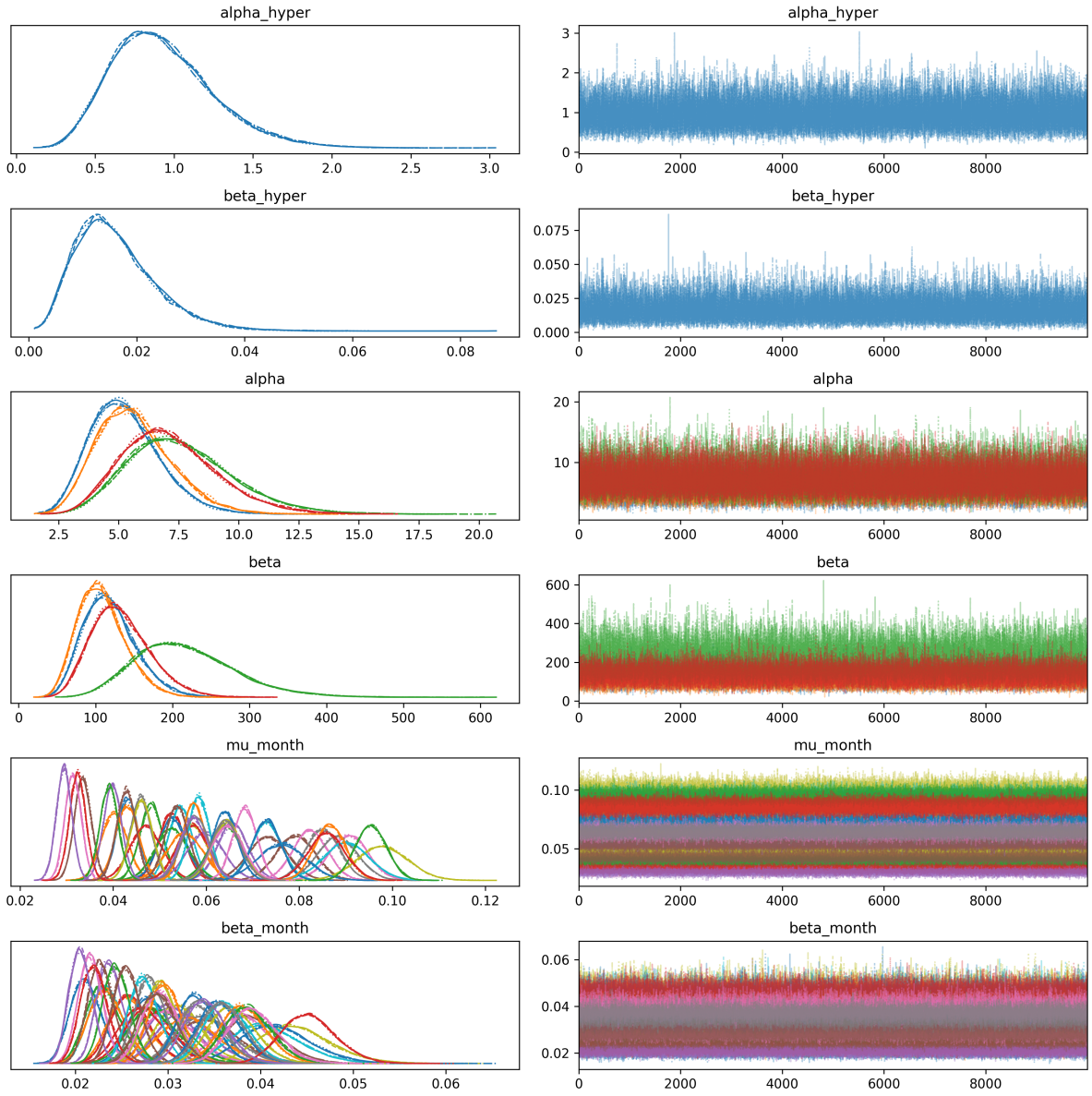

Figure 4.2: Traceplot of Markov Chains from the MCMC simulation with the Gumbel-family posterior

	mean	sd	ess_bulk	ess_tail	r_hat
τ_1	0.93	0.32	32422	27316	1
τ_2	0.02	0.01	26943	24707	1
$\Phi_{\alpha,1}$	5.26	1.44	23638	25124	1
$\Phi_{\alpha,2}$	5.65	1.56	23239	23607	1
$\Phi_{\alpha,3}$	7.6	2.19	22396	23606	1
$\Phi_{\alpha,4}$	7.12	1.97	24314	23895	1
$\Phi_{\beta,1}$	118.71	34.2	23447	24998	1
$\Phi_{\beta,2}$	108.16	31.11	23126	23236	1
$\Phi_{\beta,3}$	217.19	64.75	22060	23326	1
$\Phi_{\beta,4}$	132.86	38.15	24189	23869	1
$\phi_{v,1,1}$	0.04	0	45816	29098	1
$\phi_{v,1,2}$	0.04	0	41639	28184	1
$\phi_{v,1,3}$	0.05	0	36303	29514	1
$\phi_{v,1,4}$	0.05	0	43085	28637	1
$\phi_{v,1,5}$	0.07	0	41423	28348	1
$\phi_{v,1,6}$	0.08	0	42357	28182	1

Table 4.2: Estimated Parameters and MCMC statistics of model with Gumbel family

The dense and noisy patterns in figure 4.2 indicate that there is little-to-no dependence between observation X_{n+1} and $X_1, ..., X_n$ of drawn ZG-values from the MCMC simulation. Thus, the Markov chains are assumed to have converged. Probability density functions for the prior distributions are displayed in the left-hand column of figure 4.2. The region-specific and region-month-specific distributions are different from each other. Combined with proper convergence, this indicates that variability in the region- and month-levels are captured by the HBM.

Table 4.2 shows estimates of parameters drawn from the hyper-prior and region-specific prior distributions in the first ten rows. The rest of the rows include estimates of the parameters drawn from the region-month-specific prior distributions. The table also displays a selection of corresponding MCMC statistics. The estimated parameters represent our posterior probability distributions. Thus, we have estimated posteriors for all combinations of regions i and months t. Furthermore, the standard deviation of the

parameter estimates is close to zero when considering parameter estimates on the region-month-level of the hierarchy. This result indicates that the model "borrows strength" from the hierarchy to get accurate estimates of the posterior probability distributions. The column *r_hat* shows calculations of the Gelman-Rubin diagnostic. All diagnostic values equal 1, indicating convergence in all Markov chains of interest. The *ess_bulk* and *ess_tail* show that the effective sample sizes of the estimated parameters in the bulk and the tail of the simulated values are all at a reasonably high level.

4.3 Estimated Posterior Probability Distributions

In figure 4.3, we visualize the in-sample posterior predictive fit of the model. Data from the wind farm Nordavind A is used as in-sample data.

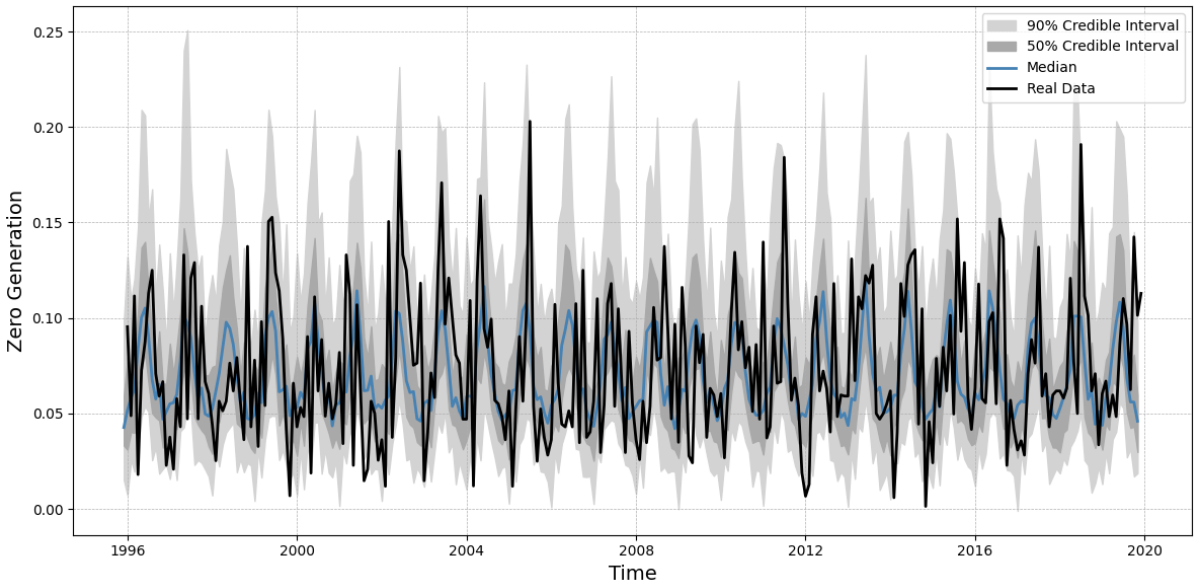

Figure 4.3: Example of the In-Sample Posterior Predictive Fit of the Estimated Posterior Distribution on data from Nordavind A

This chart shows the observed values and the median of the simulated data. The greyed-out areas define the 50% and 90% credible intervals of the MCMC simulation. These intervals represent the likelihood of the simulated values falling within a specific range. The figure shows that the model effectively captures seasonal trends, hence the spiky visuals. Periods of higher observed ZG often coincide with higher model estimates, while lower values of ZG match up with the model's lower estimates. Inspection of the chart highlights the model's ability to explain patterns in the data when assessing the risk of ZG.

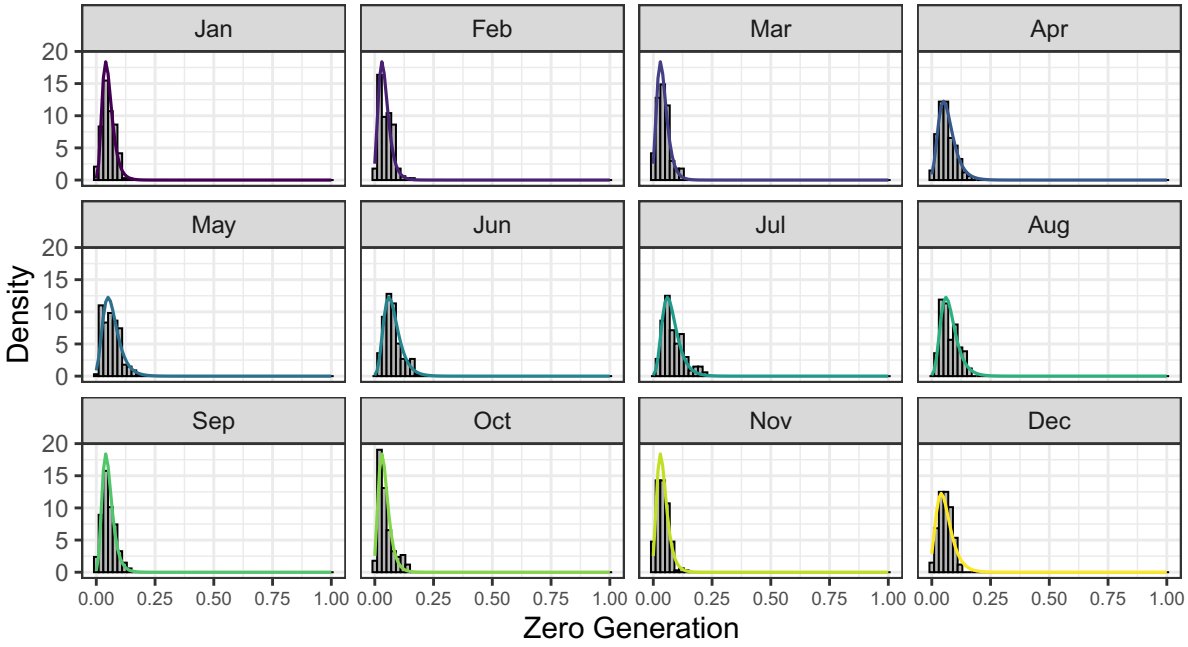

Figure 4.4: Probability Density Functions of estimated posterior probability distributions from the Gumbel-family in the Sørvest-region

Plotted probability density functions of the month-specific distributions in the Sørvest-region over histograms of observed data are presented in figure 4.4. The density of the data during the winter is more centered towards lower values than during the spring and summer. These observations coincide with the seasonal patterns in figure 2.4. The estimated posteriors and their tails adequately capture the bell shape of the distribution.

4.4 Discussion of Thresholds

Determining an appropriate trigger value is essential in parametric insurance contracts, playing a significant role for both the insurer and the insured party. Recall equation 3.4, where premiums are calculated based on the probability of ZG exceeding a predetermined trigger threshold k. Figure 4.5 shows probabilities for surpassing various thresholds specific to the Vestavind F location. In this figure, the dashed line marks an exemplary trigger value, corresponding to the 75th percentile of ZG at Vestavind F.

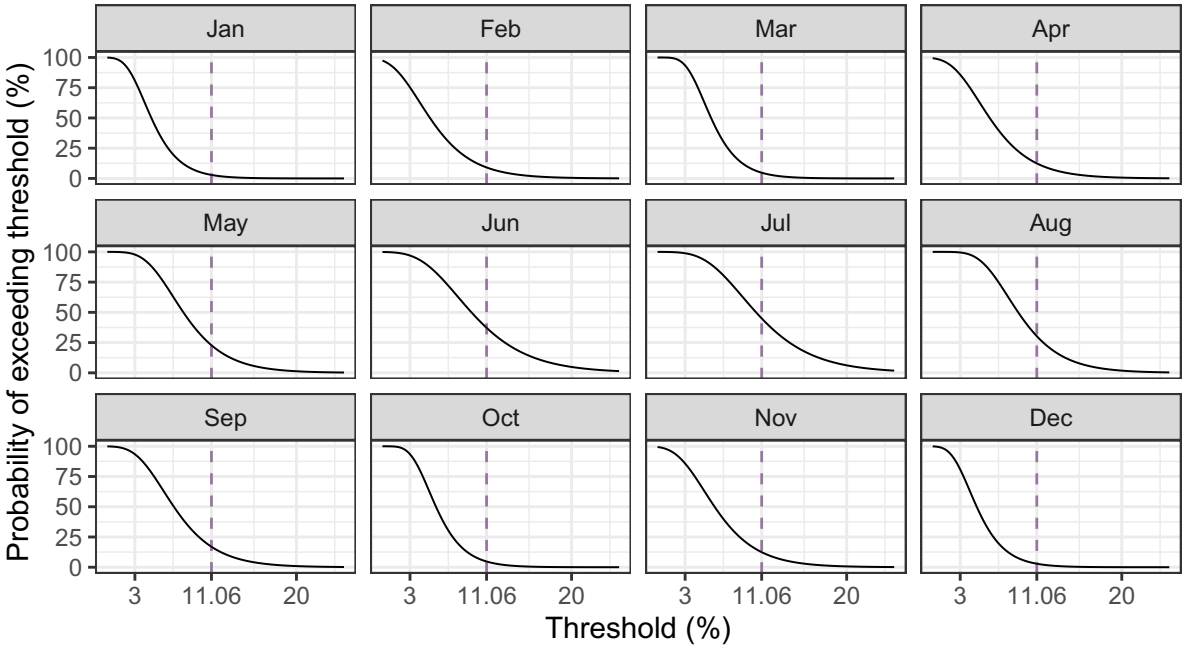

Figure 4.5: Probabilities of exceeding 75th quantile ZG for Vestavind F

The model's ability to distinguish between months is again evident, resulting in variation in the probability of ZG exceeding a threshold across different months. Specifically, we observed an increase in this probability during the summer months compared to the winter months. The peak of this trend occurs in July at this particular location, where the likelihood of surpassing the 75th quantile almost reaches 50%. Conversely, this probability approaches 0% in certain winter months.

Examining figure 4.5, it becomes apparent that adjustments in the threshold value impact the calculated premiums for the insurance contract. Specifically, opting for a higher threshold value is associated with a decreased probability of exceeding ZG, which results in more affordable premium rates for the insured. Conversely, reducing the threshold value implies a heightened probability of exceeding the threshold, resulting in more expensive premium rates. The significance of the chosen threshold for the pricing model is further elaborated upon in section 4.5.4.

4.5 Portfolio of Wind Farms

In the following section, we analyzed the impact of portfolio composition on the sum of ZG within a portfolio. We compare the *diverse* and *similar* portfolios that were defined in

section 3.3.4. We use Copula modeling to model the dependencies between the wind farms in each portfolio. CMT and p-values are calculated and compared for three different copula-families. After choosing the best performing copula family, we evaluated the risk of ZG in the portfolios using Value at Risk (VaR) and Expected Shortfall (ES).

4.5.1 Joint Probability Distributions

The method described in section 3.3.3 was used to transform data from the portfolio into uniformly distributed values from 0 to 1. Figure 4.6 displays these uniform values for a selected location, Sørvest B. An examination of the data reveals relatively uniform distributions across most months. However, results are limited by the sparse data available for specific location-month pairs. Given that only 24 data points exist for each of these combinations, certain distributions appear less consistently uniform. We assume that the transformed data follows uniform distributions.

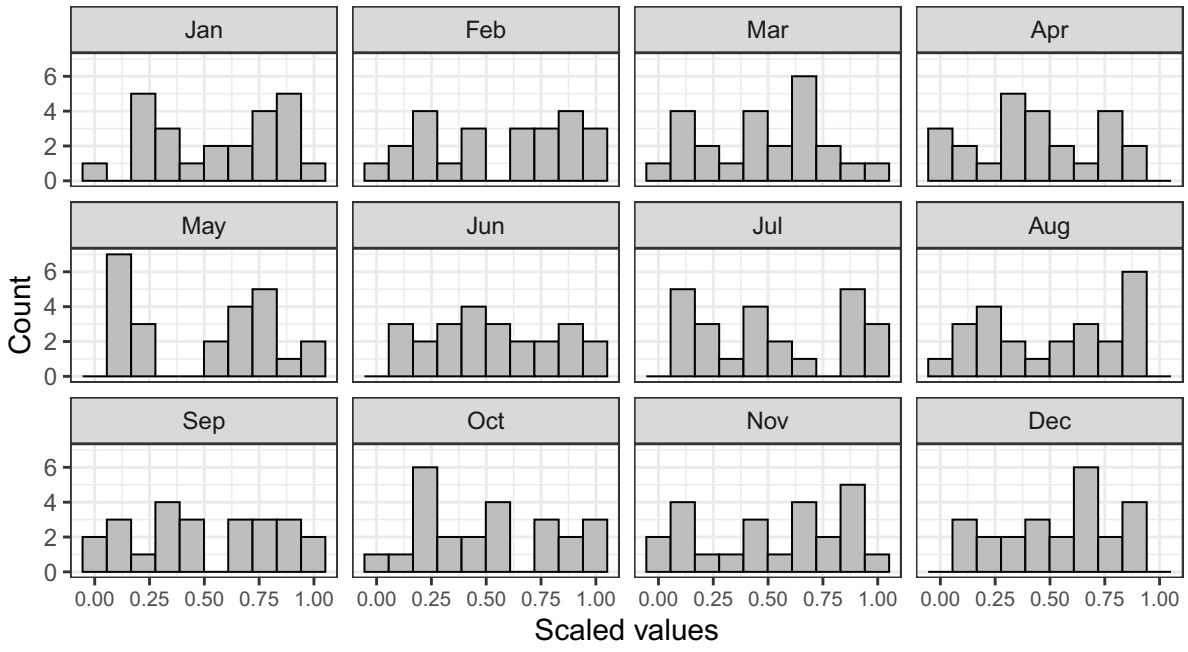

Figure 4.6: Uniform distributed values for Sørvest B

4.5.2 Goodness-of-fit Tests on Copula Families

CMT for estimated copulas of the Normal-, Joe- and Gumbel-family for the *similar* portfolio per month are shown in table 4.3a. P-values of the tests are shown in table 4.3b.

Month	Normal	Joe	Gumbel
Jan	0.06	0.14	0.08
Feb	0.06	0.09	0.06
Mar	0.04	0.11	0.06
Apr	0.04	0.13	0.07
May	0.06	0.16	0.08
Jun	0.06	0.12	0.07
Jul	0.06	0.07	0.05
Aug	0.04	0.18	0.08
Sep	0.03	0.13	0.05
Oct	0.05	0.05	0.04
Nov	0.03	0.16	0.07
Dec	0.06	0.29	0.13

(a) *CMT* estimates

Month	Normal	Joe	Gumbel
Jan	0.07	0.01	0.01
Feb	0.08	0.04	0.15
Mar	0.41	0.01	0.15
Apr	0.54	0.00	0.06
May	0.08	0.00	0.02
Jun	0.09	0.01	0.05
Jul	0.05	0.12	0.30
Aug	0.28	0.00	0.01
Sep	0.81	0.00	0.18
Oct	0.08	0.47	0.63
Nov	0.77	0.00	0.07
Dec	0.05	0.00	0.00

(b) P-values

Table 4.3: Cramér-von Mises statistics, and corresponding P-values, for estimated Normal-, Joe- & Gumbel-copulas per month

The Normal copula consistently maintains the null hypothesis H_0 across all months and exhibits the lowest CMT estimates in most of them. This result indicates that, among the copulas considered, the Normal copula most effectively captures the characteristics of the multivariate distributions. Therefore, we proceeded with our analysis using the Normal copula.

4.5.3 Evaluated Risk of Co-Dependency

After choosing the Normal-copula family, an OMC simulation was performed with $R = 10000$ iterations per month t for each portfolio. VaR and ES were calculated per month for each portfolio, and the results are presented in figure 4.7. Values on the y-axis represent the difference between 95%-VaR and ES when modeling ZG *with* or *without* co-dependence between wind farms in the portfolio. No pronounced increase in these measurements are observed when considering the *diverse* portfolio. The difference in risk seems to hover around zero, implying little to no increased risk when considering co-dependence. A risk increase is observed when considering the *similar* portfolio. ES and VaR of ZG increase

for every month when modeling *with* co-dependence. This result indicates increased risks due to co-dependence when insuring geographically close wind farms.

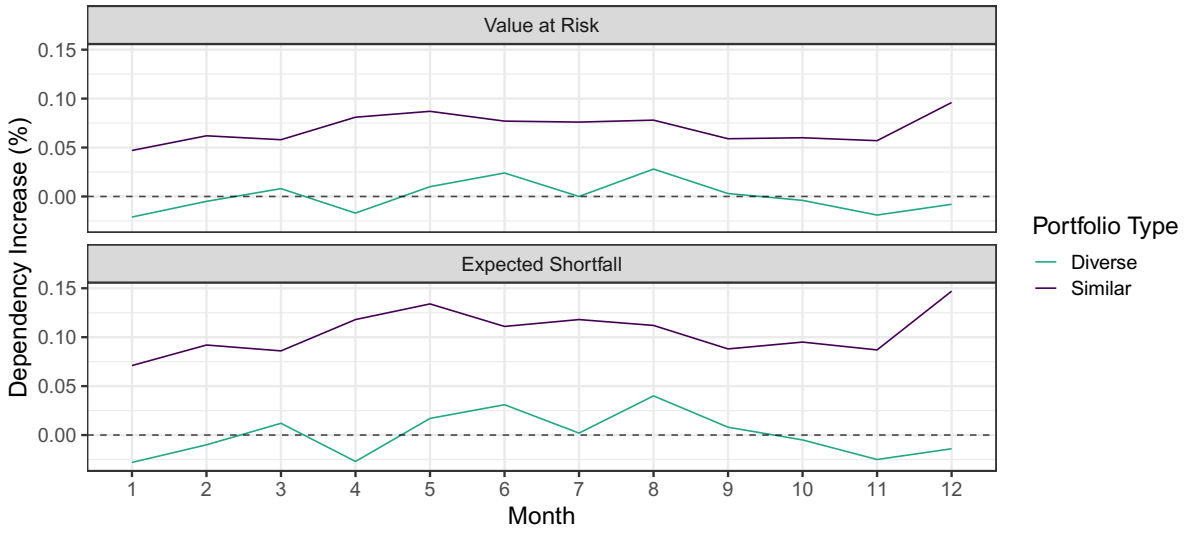

Figure 4.7: Dependency Increase when insuring a Similar Portfolio vs. a Diverse Portfolio

4.5.4 Evaluation of Monthly & Yearly Portfolio Contracts

In the final phase of our evaluation, we focused on assessing the computed premiums for the monthly and yearly portfolio contracts detailed in section 3.3.3. In Figure 4.8, histograms compare the sums of ZG for all scenarios defined in section 3.3.5. Notably, the *similar* portfolio, when modeled *with* dependence (1), exhibits more pronounced tail behavior compared to its counterpart (2) under independence. This observation suggests a more significant variability, as evidenced by a broader distribution. Additionally, a broader distribution indicates that the dependence model potentially captures more extreme values, reflecting a higher risk or more potential for variability in output within the *similar* portfolio. When examining the *diverse* portfolio, it is observed that the distributions under both dependent (3) and independent (4) scenarios are alike. This similarity indicates that co-dependency between wind farm locations within a *diverse* portfolio does not contribute to the overall risk profile.

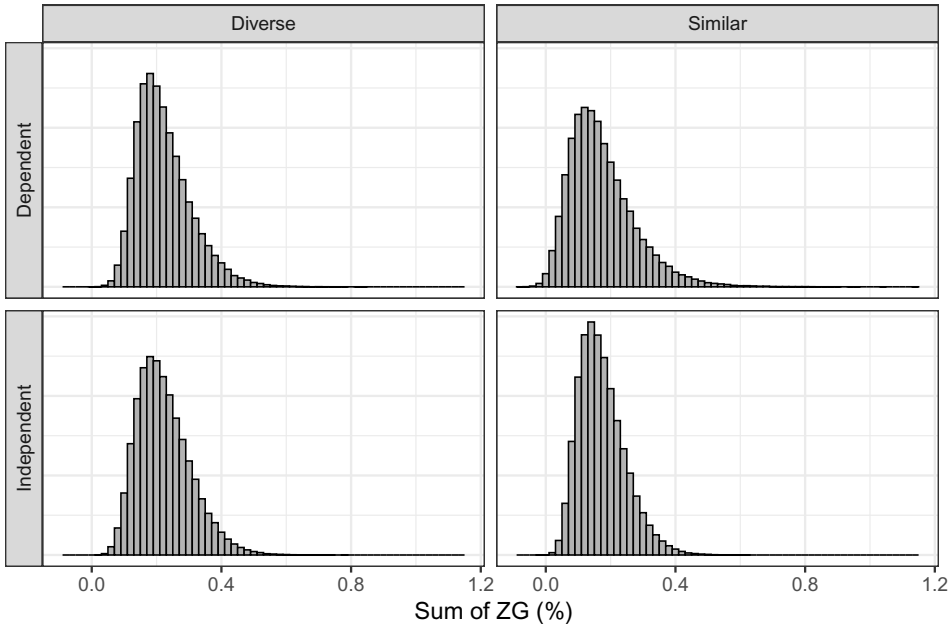

Figure 4.8: Histogram of the Sum of ZG for the Diverse & Similar portfolio, modelled with dependence & independence between wind farm locations, for all months

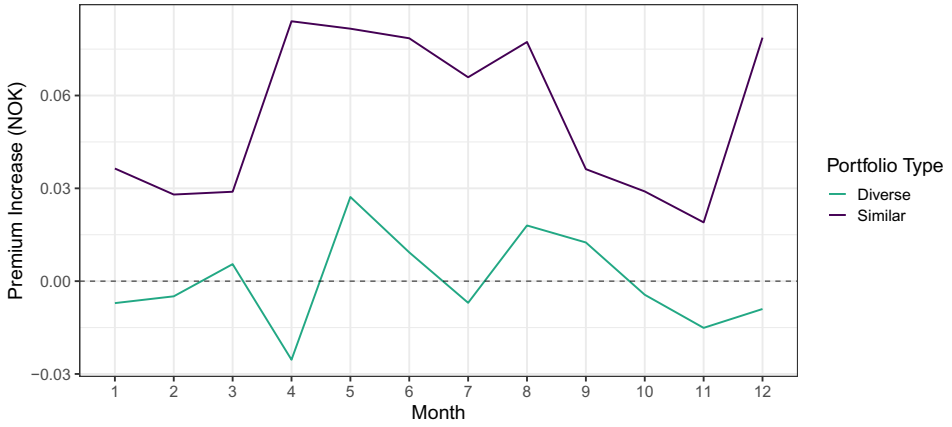

Figure 4.9: Monthly premium increase when modelling with dependence vs independence for the Diverse & Similar portfolios

Figure 4.9 presents the difference in monthly premiums modeling with dependence and and independence for the *diverse* and *similar* portfolios, given a payout of $L = 1$ NOK. The chart reveals significant variations in premiums between the two portfolios. These differences are further accentuated when considering the impact of dependence. Notably, the *similar* portfolio exhibits substantial premium hikes, particularly from April to September. This trend underscores the influence of portfolio composition on premium rates, highlighting the heightened risk and cost implications associated with more homogeneous portfolios.

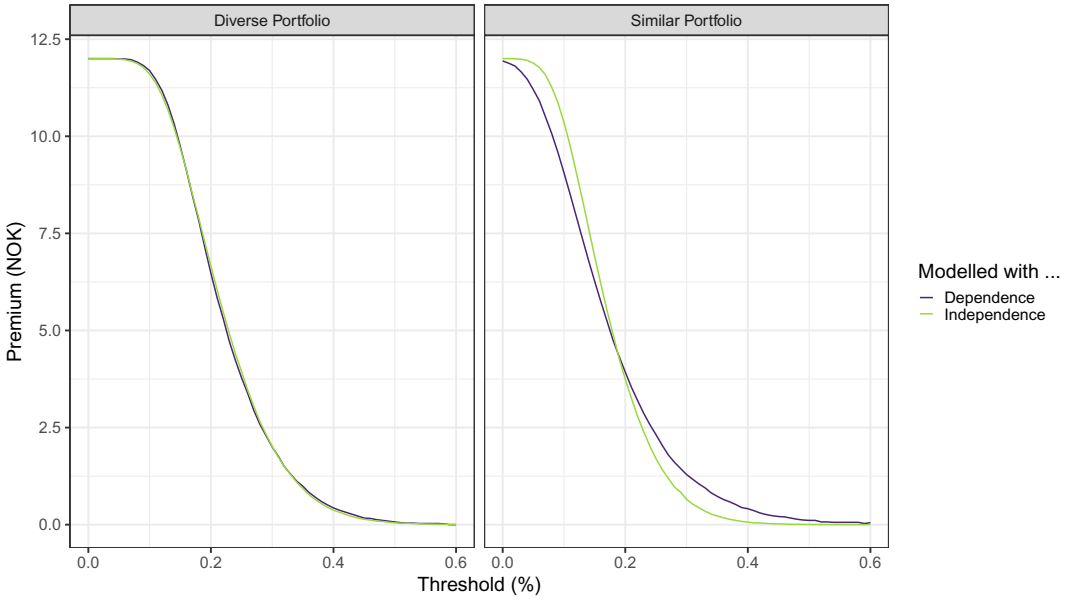

Figure 4.10: Premium as a function of trigger event threshold for all scenarios (ref. section 3.3.5)

The annual premium was calculated as described in section 3.3.5. Figure 4.10 illustrates the annual premium relative to the threshold k. As anticipated, the premium appears consistent across the models with and without dependency for the *diverse* portfolio (3) (4). Notably, the premiums for the *similar* portfolios exhibit a dependency-related discrepancy. Incorporating dependency in the wind farm locations within the portfolio results in a lower premium for smaller thresholds. In contrast, for thresholds at approximately 19% or higher, the premium for the *similar* portfolio modelled with co-dependence (1) exceeds that of the *similar* portfolio modelled without co-dependence (2).

Modeling geographically similar portfolios without co-dependence (2) leads to overestimated premiums at low threshold values and underestimated premiums at higher thresholds. Modeling with co-dependence (1) captures the tail behavior seen in figure 4.8. This result is due to the model's ability to estimate simultaneous high and simultaneous low ZG events at wind farms close to one another. Thus, it is crucial to model the insurance price based on joint distributions for the portfolio instead of independent marginal distributions per wind farm.

4.6 Limitations and Further Research

Our analysis focuses on regional and monthly resolution data, limiting our explanatory factors for ZG variability to these two dimensions. This approach has limitations, as using higher-resolution data could unveil more nuanced patterns. Another limitation of the analysis is the assumption of independence in ZG between months.

Future research should mainly involve improvements in the modeling of ZG. Improvements include using more explanatory variables for explaining ZG, increasing the resolution of our data, and employing more advanced methods for estimating ZG. Another possibility could be to research the added value of using more sophisticated weather forecasting systems to model ZG.

Secondly, future research should examine the specific loss operators that offshore wind farms experience due to ZG. This analysis would be valuable for calculating the insurance coverage of the parametric insurance model.

Our parametric insurance product is activated by a trigger event encompassing two distinct scenarios: the absence of electricity production due to either too low or excessively high wind speeds. For the insurance company, distinguishing between these two scenarios could be beneficial. This distinction represents a promising area for further research, as understanding each scenario's specific impacts and frequency could lead to more tailored insurance strategies.

5 Conclusion

In this thesis, we have proposed a pricing model for parametric insurance of zero generation events at offshore wind farm locations on the Norwegian shelf. The approach uses historical data. The research introduces a pricing strategy that would secure revenue streams for operators, making investments in the offshore wind sector more attractive. We developed two models: one for insuring a single wind farm location and another for insuring a portfolio of multiple wind farms.

We used a Hierarchical Bayesian approach to analyze the monthly and regional variability in zero generation events at offshore wind farms. Our approach utilized Markov Chain Monte Carlo simulations to estimate posterior Gumbel distributions of zero generation events, explaining monthly and regional patterns. Copulas were used to model co-dependency between wind farms within the same portfolio. Value-at-Risk and Expected Shortfall were utilized to evaluate the risk associated with insuring a portfolio of wind farms.

A fundamental discovery in our research is the heightened risk associated with insuring a portfolio of geographically proximate wind farms due to co-dependency. This result is evidenced by a pronounced increase in tail behavior and increases in Value-at-Risk and Expected Shortfall when modeling with co-dependence. Conversely, we did not observe increases in risk when comparing ZG for a geographically diverse portfolio modeling with co-dependence versus modeling without co-dependence.

Additionally, our analysis of yearly premiums for portfolios of wind farms based on a trigger event threshold revealed a notable trend. Specifically, in the scenario with a *similar* portfolio modeled *with* co-dependence (1), premiums were lower than in the scenario with a *similar* portfolio modeled *without* co-dependence (2) up to a certain threshold, beyond which the trend reversed. This pattern coincides with the broader distribution observed in co-dependency modeling, which accounts for extreme high or low zero generation events occurring simultaneously in correlated portfolios.

Considering these findings, our research shows that insurance companies can effectively price parametric insurance products for multiple wind farm locations using our proposed pricing strategy.

References

Alfsvåg, H. H. and Sollie, S. (2023). Optimal Allocation of Norwegian Offshore Wind Power : A Copula Approach : How can a thoughtful placement of offshore wind parks reduce variability in production output? Master's thesis. Accepted: 2023-10-05T07:52:51Z.

Andrew Gelman and Jennifer Hill (2007). Data Analysis Using Regression and Multilevel/Hierarchial Models. page 158. Cambridge University Press.

Beate Drewing and François Lanavère (2021). When the Wind Blows; the Role of Parametric Insurance in Renewable Energy.

Berliner, L. M. (1996). Hierarchical Bayesian Time Series Models. In Hanson, K. M. and Silver, R. N., editors, *Maximum Entropy and Bayesian Methods*, Fundamental Theories of Physics, pages 15–22, Dordrecht. Springer Netherlands.

Betancourt, M. (2018). A Conceptual Introduction to Hamiltonian Monte Carlo. arXiv:1701.02434 [stat].

Bhaumik, S. K. (2008). Reforming Indian Agriculture: Towards Employment Generation and Poverty Reduction Essays in Honour of G K Chadha. In *Reforming Indian Agriculture: Towards Employment Generation and Poverty Reduction Essays in Honour of G K Chadha*, pages 161–190. SAGE Publications India. Google-Books-ID: dLOGAwAAQBAJ.

Bozorgzadeh, N. and Bathurst, R. J. (2022). Hierarchical Bayesian approaches to statistical modelling of geotechnical data. *Georisk: Assessment and Management of Risk for Engineered Systems and Geohazards*, 16(3):452–469. Publisher: Taylor & Francis _eprint: https://doi.org/10.1080/17499518.2020.1864411.

Brooks, S. (1998). Markov chain Monte Carlo method and its application. *Journal of the Royal Statistical Society: Series D (The Statistician)*, 47(1):69–100. _eprint: https://onlinelibrary.wiley.com/doi/pdf/10.1111/1467-9884.00117.

Brooks, S., Gelman, A., Jones, G., and Meng, X.-L. (2011). *Handbook of Markov Chain Monte Carlo*. CRC Press. Google-Books-ID: qfRsAIKZ4rIC.

Bürkner, P.-C. (2017). brms: An R Package for Bayesian Multilevel Models Using Stan. *Journal of Statistical Software*, 80:1–28.

Bürkner, P.-C. (2018). Advanced Bayesian Multilevel Modeling with the R Package brms. *The R Journal*, 10(1):395.

Ciucci, F. and Chen, C. (2015). Analysis of Electrochemical Impedance Spectroscopy Data Using the Distribution of Relaxation Times: A Bayesian and Hierarchical Bayesian Approach. *Electrochimica Acta*, 167:439–454.

D'Amico, G., Petroni, F., and Prattico, F. (2017). Insuring wind energy production. *Physica A: Statistical Mechanics and its Applications*, 467:542–553.

Embrechts, P., Lindskog, F., and Mcneil, A. (2003). Modelling Dependence with Copulas and Applications to Risk Management. In *Handbook of Heavy Tailed Distributions in Finance*, pages 329–384. Elsevier.

Equinor (2023). Verdens største flytende havvindpark offisielt åpnet.

FN (2023). Parisavtalen.

Genest, C., Rémillard, B., and Beaudoin, D. (2009). Goodness-of-fit tests for copulas: A review and a power study. *Insurance: Mathematics and Economics*, 44(2):199–213.

Good, I. J. (1980). Some history of the hierarchical Bayesian methodology. *Trabajos de Estadistica Y de Investigacion Operativa*, 31(1):489–519.

Grothe, O. and Schnieders, J. (2011). Spatial dependence in wind and optimal wind power allocation: A copula-based analysis. *Energy Policy*, 39(9):4742–4754. Publisher: Elsevier.

Han, X., Zhang, G., Xie, Y., Yin, J., Zhou, H., Yang, Y., Li, J., and Bai, W. (2019). Weather index insurance for wind energy. *Global Energy Interconnection*, 2(6):541–548.

Hofert, M., Kojadinovic, I., Maechler, M., Yan, J., Nešlehová, J. G., and Morger, R. fitCopula: Fitting Copulas to Data - Copula Parameter Estimation in copula: Multivariate Dependence with Copulas.

Hofert, M., Kojadinovic, I., Maechler, M., Yan, J., Nešlehová, J. G., and Morger, R. gofCopula: Goodness-of-fit Tests for Copulas in copula: Multivariate Dependence with Copulas.

J.P.Morgan (1996). RiskMetricsTM—Technical Document.

Laguna, M. and Marklund, J. (2019). *Business process modeling, simulation and design*. CRC Press, Taylor & Francis Group, Boca Raton, third edition edition.

Lee, H. (2023). Bayesian Statistics: From Concept to Data Analysis.

Lin, X. and Kwon, W. J. (2020). Application of parametric insurance in principle-compliant and innovative ways. *Risk Management and Insurance Review*, 23(2):121–150. _eprint: https://onlinelibrary.wiley.com/doi/pdf/10.1111/rmir.12146.

Lu, Z., Martin, E., and Morris, J. (2002). Bayesian Parameter Estimation in Batch Polymerisation. In Grievink, J. and van Schijndel, J., editors, *Computer Aided Chemical Engineering*, volume 10 of *European Symposium on Computer Aided Process Engineering-12*, pages 517–522. Elsevier.

Nishio, M. and Arakawa, A. (2019). Performance of Hamiltonian Monte Carlo and No-U-Turn Sampler for estimating genetic parameters and breeding values. *Genetics Selection Evolution*, 51(1):73.

NVE (2023). Identifisering av utredningsområder for havvind.

Nyagadza, B., Link to external site, t. l. w. o. i. a. n. t., and Nyauswa, T. (2019). Parametric insurance applicability in Zimbabwe: a disaster risk management perspective from selected practicing companies. *Insurance Markets and Companies*, 10(1):36–48. Num Pages: 36-48 Place: Sumy, Ukraine Publisher: Business Perspectives Ltd. Section: Articles.

Olje-og energidepartementet (2023). Tre nye havvindområde aktuelle for opning og utlysing i 2025. Publisher: regjeringen.no.

O'Sullivan, R. (2023). Offshore wind investments recovering but still "way to go" - including on supply chain.

Pai, J., Li, Y., Yang, A., and Li, C. (2022). Earthquake parametric insurance with Bayesian spatial quantile regression. *Insurance: Mathematics and Economics*, 106:1–12.

Palmer, C. J., Lawson, R. P., and Hohwy, J. (2017). Bayesian approaches to autism: Towards volatility, action, and behavior. *Psychological Bulletin*, 143(5):521–542. Place: US Publisher: American Psychological Association.

Patil, A., Huard, D., and Fonnesbeck, C. J. (2010). PyMC: Bayesian Stochastic Modelling in Python. *Journal of statistical software*, 35(4):1–81.

Peng, R. D. (2022a). *7.4 Monitoring Convergence | Advanced Statistical Computing*.

Peng, R. D. (2022b). *Advanced Statistical Computing*.

Qiu, Y., Li, Q., Pan, Y., Yang, H., and Chen, W. (2019). A scenario generation method based on the mixture vine copula and its application in the power system with wind/hydrogen production. *International Journal of Hydrogen Energy*, 44(11):5162–5170.

Radu, N. and Alexandru, F. (2022). Parametric Insurance—A Possible and Necessary Solution to Insure the Earthquake Risk of Romania. *Risks*, 10(3):59. Num Pages: 59 Place: Basel, Switzerland Publisher: MDPI AG.

Regjeringen (2022). Grønt industriløft.

Regjeringen (2023). Nå lyser regjeringen ut de første havvindområdene. Publisher: regjeringen.no.

Rockafellar, R. T. and Uryasev, S. (2000). Optimization of conditional value-at-risk. *Journal of risk*, 2:21–42. ISBN: 1465-1211 Publisher: Citeseer.

Shiffrin, R. M., Lee, M. D., Kim, W., and Wagenmakers, E.-J. (2008). A Survey of Model Evaluation Approaches With a Tutorial on Hierarchical Bayesian Methods. *Cognitive Science*, 32(8):1248–1284. _eprint: https://onlinelibrary.wiley.com/doi/pdf/10.1080/03640210802414826.

Sklar, A. (1959). Fonctions de repartition an dimensions et leurs marges. *Publ. inst. statist. univ. Paris*, 8:229–231.

Solbrekke, I. M. and Sorteberg, A. (2022a). NORA3-WP: A high-resolution offshore wind power dataset for the Baltic, North, Norwegian, and Barents Seas. *Scientific Data*, 9(1):362. Number: 1 Publisher: Nature Publishing Group.

Solbrekke, I. M. and Sorteberg, A. (2022b). Norsk havvind del 1: Vindressurs og kraftpotensial.

Song, M., Behmanesh, I., Moaveni, B., and Papadimitriou, C. (2020). Accounting for Modeling Errors and Inherent Structural Variability through a Hierarchical Bayesian Model Updating Approach: An Overview. *Sensors*, 20(14):3874. Number: 14 Publisher: Multidisciplinary Digital Publishing Institute.

Statsministerens kontor (2022). Kraftfull satsing på havvind. Publisher: regjeringen.no.

Sun, C., Bie, Z., Xie, M., and Jiang, J. (2016). Fuzzy copula model for wind speed correlation and its application in wind curtailment evaluation. *Renewable Energy*, 93:68–76.

Thakur, J., Hesamzadeh, M. R., Date, P., and Bunn, D. (2023). Pricing and hedging wind power prediction risk with binary option contracts. *Energy Economics*, 126:106960.

Vehtari, A., Gelman, A., and Gabry, J. (2017). Practical Bayesian model evaluation using leave-one-out cross-validation and WAIC. *Statistics and Computing*, 27(5):1413–1432.

Wallevik, E. H. and Klock, H. K. (2022). Analysis of Norwegian Offshore Wind Power Production : Ranking wind farm locations using a composite index method. Master's thesis. Accepted: 2023-02-14T11:41:07Z.

Wang, S., Zhang, X., and Liu, L. (2016). Multiple stochastic correlations modeling for microgrid reliability and economic evaluation using pair-copula function. *International Journal of Electrical Power & Energy Systems*, 76:44–52.

Watanabe, S. and Opper, M. (2010). Asymptotic equivalence of Bayes cross validation and widely applicable information criterion in singular learning theory. *Journal of machine learning research*, 11(12). ISBN: 1532-4435.

Wilkie, D. and Galasso, C. (2022). A Bayesian model for wind farm capacity factors. *Energy Conversion and Management*, 252:114950.

Xiao, S., Zhang, J., Ye, J., and Zheng, J. (2021). Establishing region-specific N – Vs relationships through hierarchical Bayesian modeling. *Engineering Geology*, 287:106105.

Yang, H., Qiu, J., Meng, K., Zhao, J. H., Dong, Z. Y., and Lai, M. (2016). Insurance strategy for mitigating power system operational risk introduced by wind power forecasting uncertainty. *Renewable Energy*, 89:606–615.

Appendix

A1 Traceplots

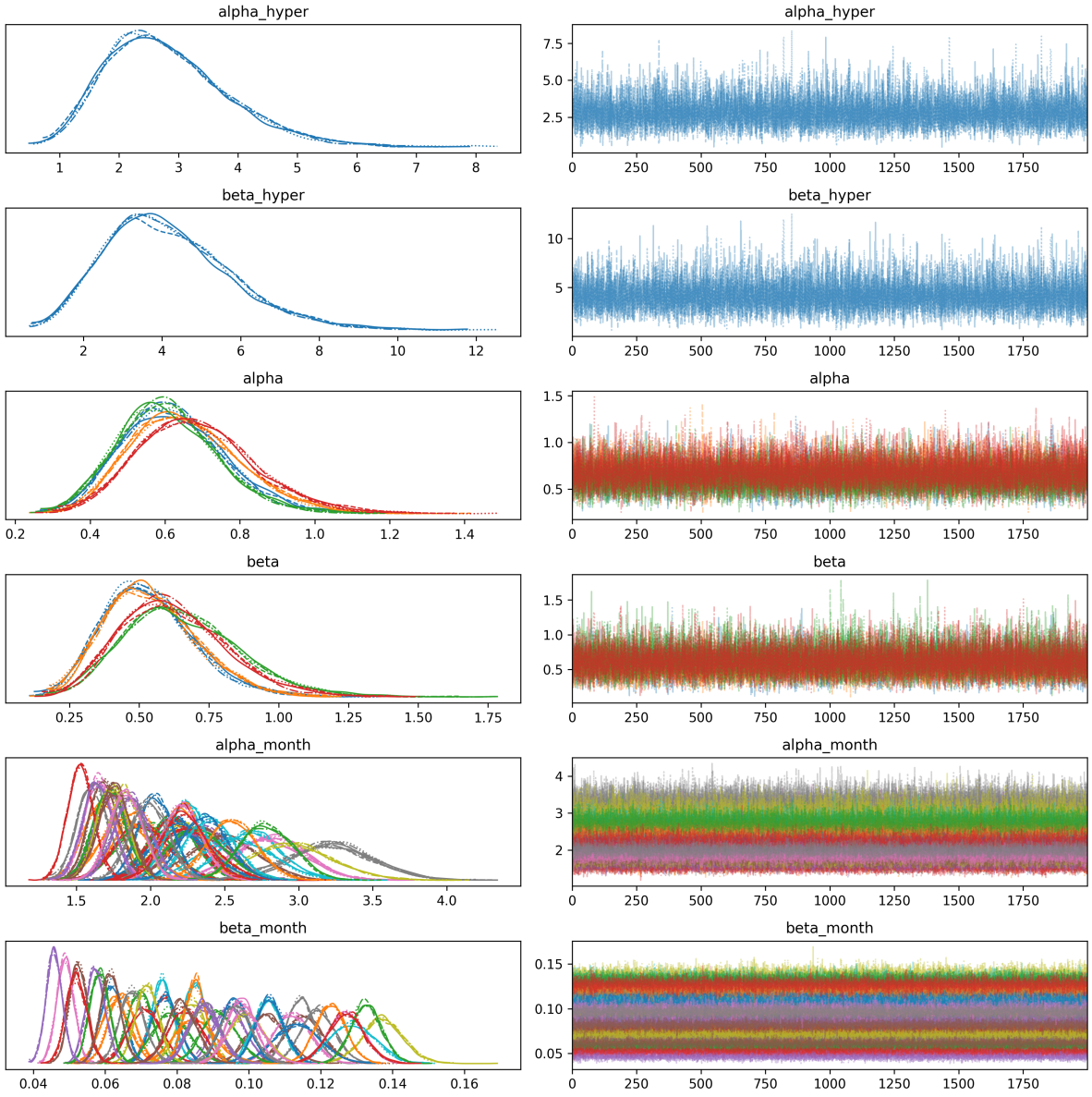

Figure A1.1: Traceplot of Markov Chains from the MCMC simulation with the Weibull-family for the posterior

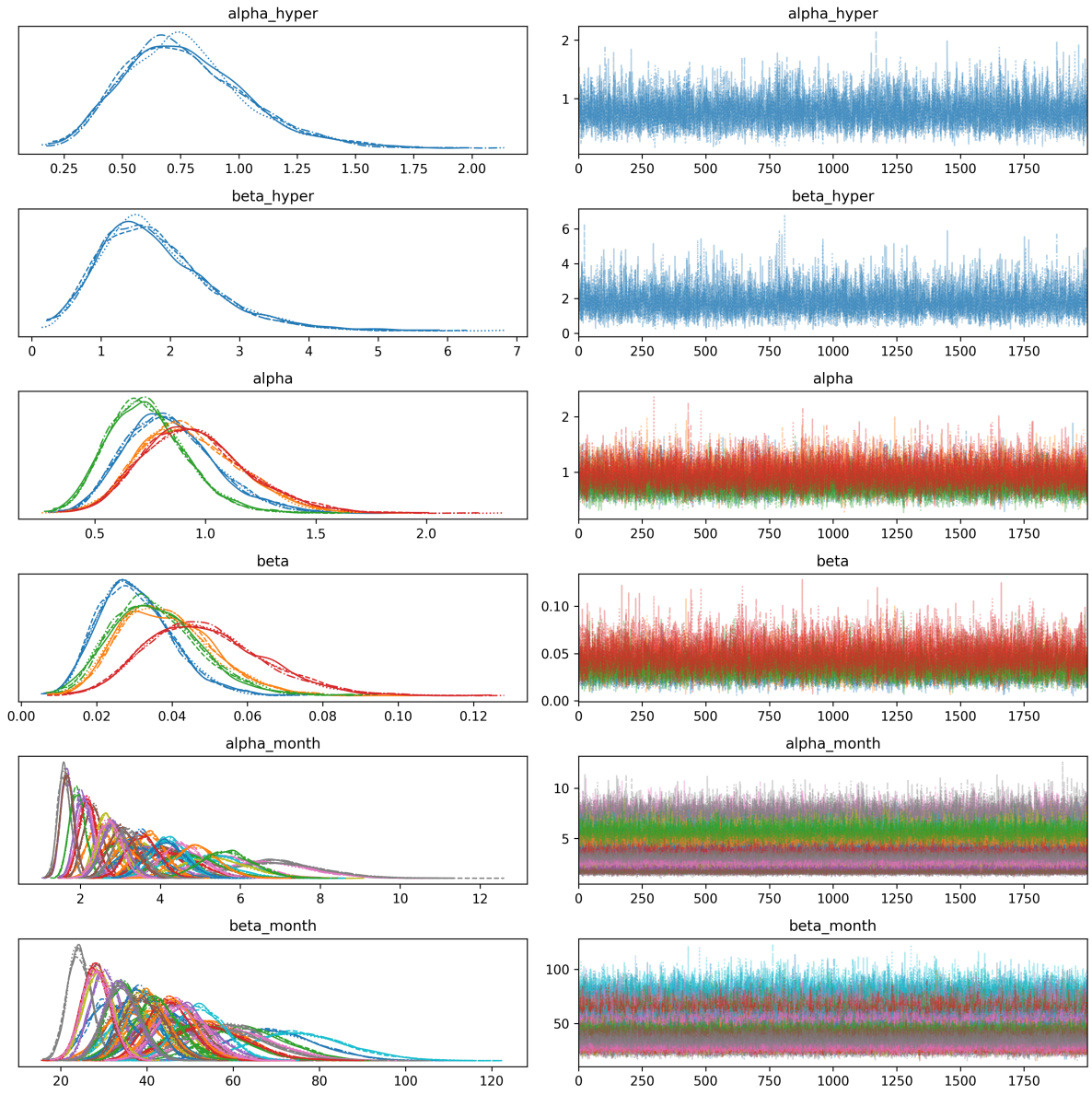

Figure A1.2: Traceplot of Markov Chains from the MCMC simulation with the Beta-family for the posterior

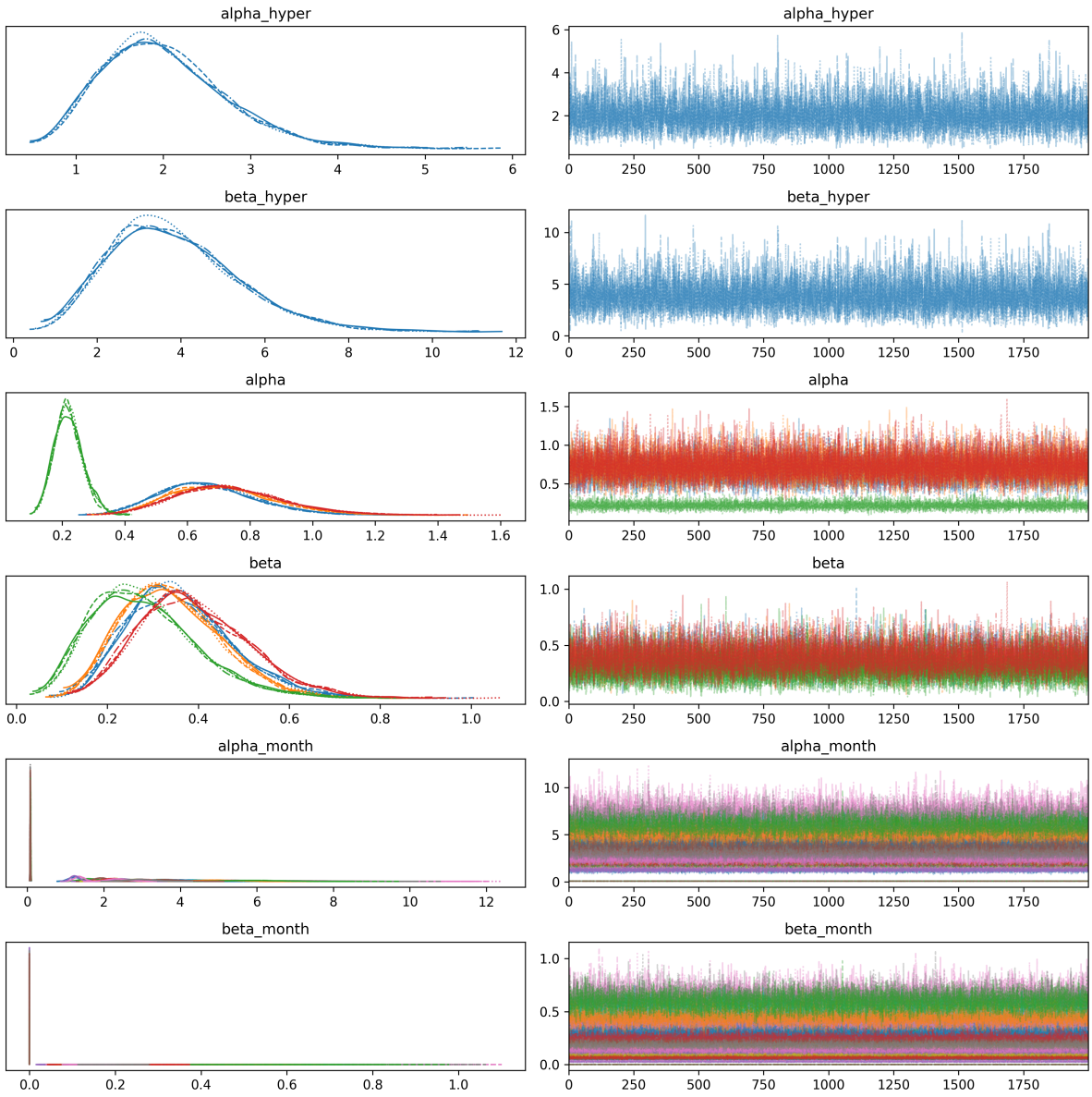

Figure A1.3: Traceplot of Markov Chains from the MCMC simulation with the Inverse Gamma-family for the posterior

A2 MCMC Parameter Estimations

Final Model

	mean	sd	hdi_3%	hdi_97%	mcse_mean	mcse_sd	ess_bulk	ess_tail	r_hat
τ_1	0.93	0.32	0.36	1.53	0	0	32422	27316	1
τ_2	0.02	0.01	0	0.03	0	0	26943	24707	1
$\Phi_{\alpha,1}$	5.26	1.44	2.73	7.99	0.01	0.01	23638	25124	1
$\Phi_{\alpha,2}$	5.65	1.56	2.92	8.61	0.01	0.01	23239	23607	1
$\Phi_{\alpha,3}$	7.6	2.19	3.83	11.78	0.01	0.01	22396	23606	1
$\Phi_{\alpha,4}$	7.12	1.97	3.63	10.86	0.01	0.01	24314	23895	1
$\Phi_{\beta,1}$	118.71	34.2	58.62	183.32	0.22	0.16	23447	24998	1
$\Phi_{\beta,2}$	108.16	31.11	53.82	167.36	0.2	0.14	23126	23236	1
$\Phi_{\beta,3}$	217.19	64.75	102.51	337.76	0.43	0.3	22060	23326	1
$\Phi_{\beta,4}$	132.86	38.15	63.9	203.22	0.24	0.17	24189	23869	1
$\phi_{v,1,1}$	0.04	0	0.04	0.05	0	0	45816	29098	1
$\phi_{v,1,2}$	0.04	0	0.04	0.05	0	0	41639	28184	1
$\phi_{v,1,3}$	0.05	0	0.04	0.05	0	0	36303	29514	1
$\phi_{v,1,4}$	0.05	0	0.05	0.06	0	0	43085	28637	1
$\phi_{v,1,5}$	0.07	0	0.06	0.07	0	0	41423	28348	1
$\phi_{v,1,6}$	0.08	0	0.07	0.09	0	0	42357	28182	1
$\phi_{v,1,7}$	0.09	0	0.08	0.1	0	0	39961	28314	1
$\phi_{v,1,8}$	0.08	0	0.08	0.09	0	0	45672	32477	1
$\phi_{v,1,9}$	0.06	0	0.05	0.06	0	0	41712	29267	1
$\phi_{v,1,10}$	0.05	0	0.05	0.06	0	0	46285	30425	1
$\phi_{v,1,11}$	0.05	0	0.05	0.06	0	0	41733	27818	1
$\phi_{v,1,12}$	0.04	0	0.04	0.05	0	0	38929	30428	1
$\phi_{v,2,1}$	0.05	0	0.05	0.06	0	0	44452	29596	1
$\phi_{v,2,2}$	0.05	0	0.04	0.05	0	0	40062	27474	1
$\phi_{v,2,3}$	0.06	0	0.05	0.07	0	0	38355	27829	1
$\phi_{v,2,4}$	0.07	0	0.06	0.08	0	0	44425	31553	1
$\phi_{v,2,5}$	0.08	0	0.08	0.09	0	0	44237	29149	1
$\phi_{v,2,6}$	0.09	0	0.08	0.1	0	0	39445	27138	1
$\phi_{v,2,7}$	0.1	0.01	0.09	0.11	0	0	40804	29344	1
$\phi_{v,2,8}$	0.09	0	0.08	0.1	0	0	39719	27734	1
$\phi_{v,2,9}$	0.08	0	0.07	0.09	0	0	46802	27602	1
$\phi_{v,2,10}$	0.06	0	0.05	0.06	0	0	39645	28452	1
$\phi_{v,2,11}$	0.06	0	0.06	0.07	0	0	46646	28738	1
$\phi_{v,2,12}$	0.06	0	0.05	0.06	0	0	44080	30174	1
$\phi_{v,3,1}$	0.04	0	0.04	0.04	0	0	43157	29906	1
$\phi_{v,3,2}$	0.03	0	0.03	0.04	0	0	42233	29729	1
$\phi_{v,3,3}$	0.03	0	0.03	0.04	0	0	46232	29714	1
$\phi_{v,3,4}$	0.05	0	0.04	0.05	0	0	39960	30788	1
$\phi_{v,3,5}$	0.05	0	0.04	0.05	0	0	40753	30612	1
$\phi_{v,3,6}$	0.06	0	0.05	0.06	0	0	42963	30487	1
$\phi_{v,3,7}$	0.06	0	0.06	0.07	0	0	48652	30272	1
$\phi_{v,3,8}$	0.06	0	0.05	0.06	0	0	43503	28748	1
$\phi_{v,3,9}$	0.04	0	0.04	0.04	0	0	45123	28974	1

$\phi_{v,3,10}$	0.03	0	0.03	0.04	0	0	38219	27750	1
$\phi_{v,3,11}$	0.03	0	0.03	0.03	0	0	35055	27915	1
$\phi_{v,3,12}$	0.04	0	0.04	0.05	0	0	43635	30458	1
$\phi_{v,4,1}$	0.07	0	0.06	0.07	0	0	43745	30288	1
$\phi_{v,4,2}$	0.06	0	0.05	0.06	0	0	43244	28651	1
$\phi_{v,4,3}$	0.06	0	0.06	0.07	0	0	45463	29143	1
$\phi_{v,4,4}$	0.07	0	0.07	0.08	0	0	45851	29198	1
$\phi_{v,4,5}$	0.07	0	0.07	0.08	0	0	46631	30455	1
$\phi_{v,4,6}$	0.09	0	0.08	0.09	0	0	42954	29010	1
$\phi_{v,4,7}$	0.1	0	0.09	0.1	0	0	46730	31639	1
$\phi_{v,4,8}$	0.09	0	0.08	0.09	0	0	40916	29422	1
$\phi_{v,4,9}$	0.06	0	0.05	0.06	0	0	41231	29453	1
$\phi_{v,4,10}$	0.05	0	0.05	0.06	0	0	44579	29037	1
$\phi_{v,4,11}$	0.06	0	0.06	0.07	0	0	44367	30432	1
$\phi_{v,4,12}$	0.06	0	0.06	0.07	0	0	40298	29126	1
$\phi_{u,1,1}$	0.02	0	0.02	0.02	0	0	44406	30208	1
$\phi_{u,1,2}$	0.03	0	0.02	0.03	0	0	46028	29929	1
$\phi_{u,1,3}$	0.02	0	0.02	0.03	0	0	40765	28597	1
$\phi_{u,1,4}$	0.03	0	0.02	0.03	0	0	45176	30327	1
$\phi_{u,1,5}$	0.03	0	0.03	0.04	0	0	43497	29315	1
$\phi_{u,1,6}$	0.04	0	0.03	0.04	0	0	44993	30988	1
$\phi_{u,1,7}$	0.04	0	0.03	0.04	0	0	42311	29640	1
$\phi_{u,1,8}$	0.03	0	0.03	0.04	0	0	45231	30382	1
$\phi_{u,1,9}$	0.03	0	0.03	0.04	0	0	44667	29837	1
$\phi_{u,1,10}$	0.02	0	0.02	0.03	0	0	41874	29133	1
$\phi_{u,1,11}$	0.03	0	0.02	0.03	0	0	43627	28254	1
$\phi_{u,1,12}$	0.02	0	0.02	0.03	0	0	37229	28970	1
$\phi_{u,2,1}$	0.03	0	0.02	0.04	0	0	39394	30270	1
$\phi_{u,2,2}$	0.03	0	0.02	0.03	0	0	41596	29907	1
$\phi_{u,2,3}$	0.03	0	0.03	0.04	0	0	36412	29284	1
$\phi_{u,2,4}$	0.04	0	0.03	0.04	0	0	41386	28598	1
$\phi_{u,2,5}$	0.03	0	0.02	0.04	0	0	40211	29820	1
$\phi_{u,2,6}$	0.03	0	0.03	0.04	0	0	44270	29852	1
$\phi_{u,2,7}$	0.04	0	0.04	0.05	0	0	43580	29237	1
$\phi_{u,2,8}$	0.04	0	0.03	0.05	0	0	43678	30072	1
$\phi_{u,2,9}$	0.04	0	0.04	0.05	0	0	46242	29695	1
$\phi_{u,2,10}$	0.03	0	0.03	0.04	0	0	46272	30885	1
$\phi_{u,2,11}$	0.03	0	0.02	0.03	0	0	45440	29025	1
$\phi_{u,2,12}$	0.03	0	0.02	0.03	0	0	45373	29772	1
$\phi_{u,3,1}$	0.02	0	0.02	0.03	0	0	42446	29673	1
$\phi_{u,3,2}$	0.02	0	0.02	0.02	0	0	47021	30322	1
$\phi_{u,3,3}$	0.02	0	0.02	0.02	0	0	40665	29533	1
$\phi_{u,3,4}$	0.03	0	0.02	0.03	0	0	44869	29968	1
$\phi_{u,3,5}$	0.03	0	0.03	0.03	0	0	42386	31057	1
$\phi_{u,3,6}$	0.03	0	0.02	0.03	0	0	41653	30156	1
$\phi_{u,3,7}$	0.03	0	0.03	0.04	0	0	43076	29152	1
$\phi_{u,3,8}$	0.03	0	0.03	0.03	0	0	46290	30596	1
$\phi_{u,3,9}$	0.02	0	0.02	0.03	0	0	40616	30889	1
$\phi_{u,3,10}$	0.02	0	0.02	0.02	0	0	41301	30802	1

$\phi_{u,3,11}$	0.02	0	0.02	0.02	0	0	38444	29495	1
$\phi_{u,3,12}$	0.03	0	0.02	0.03	0	0	45240	30096	1
$\phi_{u,4,1}$	0.03	0	0.03	0.03	0	0	43693	30385	1
$\phi_{u,4,2}$	0.03	0	0.03	0.04	0	0	44730	30409	1
$\phi_{u,4,3}$	0.04	0	0.03	0.04	0	0	46908	30907	1
$\phi_{u,4,4}$	0.04	0	0.03	0.04	0	0	45262	30463	1
$\phi_{u,4,5}$	0.04	0	0.03	0.04	0	0	44305	28464	1
$\phi_{u,4,6}$	0.04	0	0.03	0.04	0	0	39470	30709	1
$\phi_{u,4,7}$	0.04	0	0.03	0.04	0	0	44606	31071	1
$\phi_{u,4,8}$	0.04	0	0.04	0.05	0	0	48635	31012	1
$\phi_{u,4,9}$	0.03	0	0.03	0.04	0	0	48790	30512	1
$\phi_{u,4,10}$	0.03	0	0.02	0.03	0	0	40087	28966	1
$\phi_{u,4,11}$	0.04	0	0.03	0.04	0	0	42460	29707	1
$\phi_{u,4,12}$	0.04	0	0.03	0.04	0	0	44559	30083	1

Weibull - Model Comparison

	mean	sd	hdi_3%	hdi_97%	mcse_mean	mcse_sd	ess_bulk	ess_tail	r_hat
τ_1	2.82	1.04	1.06	4.75	0.01	0.01	13088	6581	1
τ_2	4.17	1.63	1.4	7.25	0.01	0.01	14564	5972	1
$\Phi_{\alpha,1}$	0.62	0.14	0.37	0.88	0	0	13277	6179	1
$\Phi_{\alpha,2}$	0.66	0.15	0.4	0.93	0	0	13036	6295	1
$\Phi_{\alpha,3}$	0.61	0.13	0.36	0.86	0	0	13525	6382	1
$\Phi_{\alpha,4}$	0.68	0.16	0.4	0.97	0	0	13778	6353	1
$\Phi_{\beta,1}$	0.54	0.16	0.23	0.84	0	0	13966	6197	1
$\Phi_{\beta,2}$	0.54	0.17	0.25	0.87	0	0	14132	5933	1
$\Phi_{\beta,3}$	0.66	0.2	0.31	1.06	0	0	12795	6362	1
$\Phi_{\beta,4}$	0.62	0.19	0.29	0.99	0	0	13750	6317	1
$\phi_{v,1,1}$	2.16	0.16	1.85	2.45	0	0	15617	6734	1
$\phi_{v,1,2}$	1.68	0.13	1.43	1.92	0	0	15094	6417	1
$\phi_{v,1,3}$	2.14	0.16	1.84	2.44	0	0	16373	5489	1
$\phi_{v,1,4}$	2.16	0.16	1.86	2.46	0	0	16276	6287	1
$\phi_{v,1,5}$	2.34	0.18	2	2.67	0	0	16749	6047	1
$\phi_{v,1,6}$	2.34	0.18	2	2.69	0	0	15040	6204	1
$\phi_{v,1,7}$	2.84	0.23	2.42	3.26	0	0	14372	6081	1
$\phi_{v,1,8}$	3.24	0.26	2.74	3.74	0	0	13873	6675	1
$\phi_{v,1,9}$	2.23	0.18	1.9	2.56	0	0	13619	5241	1
$\phi_{v,1,10}$	2.68	0.21	2.28	3.05	0	0	14489	5708	1
$\phi_{v,1,11}$	2.2	0.17	1.88	2.52	0	0	15592	6046	1
$\phi_{v,1,12}$	1.92	0.14	1.65	2.19	0	0	15321	6173	1
$\phi_{v,2,1}$	1.97	0.18	1.64	2.29	0	0	15617	6566	1
$\phi_{v,2,2}$	1.95	0.18	1.63	2.29	0	0	12843	6544	1
$\phi_{v,2,3}$	2.3	0.21	1.9	2.7	0	0	14561	6145	1
$\phi_{v,2,4}$	2.5	0.23	2.07	2.92	0	0	15076	6274	1
$\phi_{v,2,5}$	2.79	0.25	2.35	3.27	0	0	14827	5637	1
$\phi_{v,2,6}$	3.2	0.3	2.65	3.76	0	0	15551	6323	1
$\phi_{v,2,7}$	2.95	0.28	2.41	3.46	0	0	15306	6154	1
$\phi_{v,2,8}$	2.58	0.24	2.15	3.04	0	0	15211	6010	1
$\phi_{v,2,9}$	2.2	0.21	1.82	2.59	0	0	14536	5909	1
$\phi_{v,2,10}$	1.83	0.16	1.54	2.14	0	0	14715	5549	1
$\phi_{v,2,11}$	2.31	0.2	1.93	2.66	0	0	14611	6279	1
$\phi_{v,2,12}$	2.25	0.19	1.9	2.63	0	0	15262	6304	1
$\phi_{v,3,1}$	1.73	0.11	1.51	1.94	0	0	15718	6398	1
$\phi_{v,3,2}$	1.69	0.1	1.48	1.87	0	0	12264	6231	1
$\phi_{v,3,3}$	1.65	0.1	1.47	1.85	0	0	14368	6007	1
$\phi_{v,3,4}$	1.61	0.1	1.41	1.8	0	0	16306	5847	1
$\phi_{v,3,5}$	1.84	0.11	1.63	2.05	0	0	16664	6447	1
$\phi_{v,3,6}$	2.24	0.13	2	2.48	0	0	13590	6110	1
$\phi_{v,3,7}$	2.04	0.12	1.82	2.27	0	0	16011	6005	1
$\phi_{v,3,8}$	2.22	0.13	1.97	2.48	0	0	17778	5938	1
$\phi_{v,3,9}$	1.72	0.11	1.52	1.93	0	0	14877	6392	1
$\phi_{v,3,10}$	1.53	0.09	1.37	1.7	0	0	14943	6392	1
$\phi_{v,3,11}$	1.64	0.1	1.46	1.84	0	0	14253	5718	1

$\phi_{v,3,12}$	1.75	0.12	1.54	1.97	0	0	15283	6039	1
$\phi_{v,4,1}$	2.21	0.13	1.96	2.45	0	0	15179	6199	1
$\phi_{v,4,2}$	1.85	0.12	1.63	2.06	0	0	14165	6812	1
$\phi_{v,4,3}$	1.75	0.1	1.55	1.95	0	0	16170	5833	1
$\phi_{v,4,4}$	2.4	0.16	2.11	2.7	0	0	17198	5687	1
$\phi_{v,4,5}$	2.37	0.16	2.08	2.66	0	0	16470	6545	1
$\phi_{v,4,6}$	2.55	0.16	2.25	2.86	0	0	14357	6128	1
$\phi_{v,4,7}$	2.79	0.18	2.45	3.11	0	0	15375	6662	1
$\phi_{v,4,8}$	2.23	0.15	1.95	2.5	0	0	13615	6093	1
$\phi_{v,4,9}$	1.88	0.12	1.64	2.09	0	0	14243	5632	1
$\phi_{v,4,10}$	1.76	0.1	1.56	1.94	0	0	14104	6408	1
$\phi_{v,4,11}$	1.84	0.12	1.63	2.06	0	0	12682	6356	1
$\phi_{v,4,12}$	1.99	0.12	1.76	2.22	0	0	13207	6072	1
$\phi_{u,1,1}$	0.06	0	0.06	0.07	0	0	15289	5980	1
$\phi_{u,1,2}$	0.06	0	0.06	0.07	0	0	12207	5913	1
$\phi_{u,1,3}$	0.07	0	0.06	0.08	0	0	14906	6515	1
$\phi_{u,1,4}$	0.08	0	0.07	0.08	0	0	14267	6319	1
$\phi_{u,1,5}$	0.1	0	0.09	0.1	0	0	15223	6295	1
$\phi_{u,1,6}$	0.12	0	0.11	0.13	0	0	14876	5450	1
$\phi_{u,1,7}$	0.13	0	0.12	0.14	0	0	13968	5697	1
$\phi_{u,1,8}$	0.12	0	0.11	0.12	0	0	13447	5822	1
$\phi_{u,1,9}$	0.08	0	0.08	0.09	0	0	13549	6714	1
$\phi_{u,1,10}$	0.08	0	0.07	0.08	0	0	16163	6695	1
$\phi_{u,1,11}$	0.08	0	0.07	0.08	0	0	13364	6697	1
$\phi_{u,1,12}$	0.06	0	0.06	0.07	0	0	12457	5950	1
$\phi_{u,2,1}$	0.08	0	0.07	0.09	0	0	13712	5979	1
$\phi_{u,2,2}$	0.07	0	0.06	0.08	0	0	15724	6303	1
$\phi_{u,2,3}$	0.09	0	0.08	0.1	0	0	14760	6446	1
$\phi_{u,2,4}$	0.1	0	0.1	0.12	0	0	14230	6656	1
$\phi_{u,2,5}$	0.11	0	0.1	0.12	0	0	14396	6197	1
$\phi_{u,2,6}$	0.12	0	0.11	0.13	0	0	15252	6432	1
$\phi_{u,2,7}$	0.14	0.01	0.13	0.15	0	0	14918	5998	1
$\phi_{u,2,8}$	0.13	0.01	0.12	0.14	0	0	14651	6064	1
$\phi_{u,2,9}$	0.11	0.01	0.1	0.12	0	0	14230	6481	1
$\phi_{u,2,10}$	0.08	0.01	0.07	0.1	0	0	14262	6465	1
$\phi_{u,2,11}$	0.09	0	0.08	0.1	0	0	13328	6499	1
$\phi_{u,2,12}$	0.08	0	0.07	0.09	0	0	16988	6465	1
$\phi_{u,3,1}$	0.06	0	0.05	0.06	0	0	14850	6033	1
$\phi_{u,3,2}$	0.05	0	0.05	0.06	0	0	14998	5819	1
$\phi_{u,3,3}$	0.05	0	0.04	0.05	0	0	14063	6366	1
$\phi_{u,3,4}$	0.07	0	0.06	0.07	0	0	15390	5782	1
$\phi_{u,3,5}$	0.07	0	0.06	0.08	0	0	16490	6360	1
$\phi_{u,3,6}$	0.08	0	0.08	0.09	0	0	14869	6398	1
$\phi_{u,3,7}$	0.1	0	0.09	0.1	0	0	16920	6387	1
$\phi_{u,3,8}$	0.08	0	0.08	0.09	0	0	14134	6545	1
$\phi_{u,3,9}$	0.06	0	0.05	0.06	0	0	14468	6439	1
$\phi_{u,3,10}$	0.05	0	0.05	0.06	0	0	16250	6528	1
$\phi_{u,3,11}$	0.05	0	0.04	0.05	0	0	13779	6109	1
$\phi_{u,3,12}$	0.06	0	0.06	0.07	0	0	15859	6437	1

$\phi_{u,4,1}$	0.1	0	0.09	0.1	0	0	16058	6114	1
$\phi_{u,4,2}$	0.09	0	0.08	0.1	0	0	15557	5962	1
$\phi_{u,4,3}$	0.1	0	0.09	0.11	0	0	14021	6355	1
$\phi_{u,4,4}$	0.1	0	0.1	0.11	0	0	14772	6258	1
$\phi_{u,4,5}$	0.11	0	0.1	0.11	0	0	14123	5974	1
$\phi_{u,4,6}$	0.12	0	0.12	0.13	0	0	13794	6164	1
$\phi_{u,4,7}$	0.13	0	0.12	0.14	0	0	13357	5699	1
$\phi_{u,4,8}$	0.13	0	0.12	0.14	0	0	16120	6013	1
$\phi_{u,4,9}$	0.09	0	0.08	0.1	0	0	15926	5657	1
$\phi_{u,4,10}$	0.08	0	0.07	0.09	0	0	16067	6867	1
$\phi_{u,4,11}$	0.1	0	0.09	0.11	0	0	14914	5858	1
$\phi_{u,4,12}$	0.1	0	0.09	0.1	0	0	18378	6276	1

Gumbel - Model Comparison

	mean	sd	hdi_3%	hdi_97%	mcse_mean	mcse_sd	ess_bulk	ess_tail	r_hat
τ_1	0.93	0.33	0.37	1.54	0	0	8762	5732	1
τ_2	0.02	0.01	0	0.03	0	0	7825	5371	1
$\Phi_{\alpha,1}$	5.25	1.44	2.61	7.91	0.02	0.01	8247	5816	1
$\Phi_{\alpha,2}$	5.64	1.57	2.96	8.7	0.02	0.01	6694	4967	1
$\Phi_{\alpha,3}$	7.6	2.18	3.88	11.81	0.03	0.02	7129	5781	1
$\Phi_{\alpha,4}$	7.12	2.02	3.64	10.98	0.02	0.02	6986	5109	1
$\Phi_{\beta,1}$	118.42	34.15	57.65	182.16	0.38	0.28	8173	5692	1
$\Phi_{\beta,2}$	107.99	31.53	52.95	168.81	0.37	0.26	6911	5166	1
$\Phi_{\beta,3}$	216.6	64.81	105.57	342.35	0.76	0.55	7136	5781	1
$\Phi_{\beta,4}$	132.98	39.1	64.8	206.02	0.46	0.34	7165	5402	1
$\phi_{v,1,1}$	0.04	0	0.04	0.05	0	0	10399	6318	1
$\phi_{v,1,2}$	0.04	0	0.04	0.04	0	0	10261	5730	1
$\phi_{v,1,3}$	0.05	0	0.04	0.05	0	0	10571	6116	1
$\phi_{v,1,4}$	0.05	0	0.05	0.06	0	0	11632	6178	1
$\phi_{v,1,5}$	0.07	0	0.06	0.07	0	0	10409	6133	1
$\phi_{v,1,6}$	0.08	0	0.07	0.09	0	0	11137	6056	1
$\phi_{v,1,7}$	0.09	0	0.08	0.1	0	0	11078	6094	1
$\phi_{v,1,8}$	0.08	0	0.08	0.09	0	0	11347	6440	1
$\phi_{v,1,9}$	0.06	0	0.05	0.06	0	0	9227	5673	1
$\phi_{v,1,10}$	0.05	0	0.05	0.06	0	0	11354	5871	1
$\phi_{v,1,11}$	0.05	0	0.05	0.06	0	0	9926	6247	1
$\phi_{v,1,12}$	0.04	0	0.04	0.05	0	0	9674	6130	1
$\phi_{v,2,1}$	0.05	0	0.05	0.06	0	0	9443	5821	1
$\phi_{v,2,2}$	0.05	0	0.04	0.05	0	0	8650	5499	1
$\phi_{v,2,3}$	0.06	0	0.05	0.07	0	0	10377	5749	1
$\phi_{v,2,4}$	0.07	0	0.06	0.08	0	0	9631	6128	1
$\phi_{v,2,5}$	0.08	0	0.08	0.09	0	0	8974	6032	1
$\phi_{v,2,6}$	0.09	0	0.08	0.1	0	0	10342	5964	1
$\phi_{v,2,7}$	0.1	0.01	0.09	0.11	0	0	10928	5578	1
$\phi_{v,2,8}$	0.09	0	0.08	0.1	0	0	10009	5189	1
$\phi_{v,2,9}$	0.08	0	0.07	0.09	0	0	9594	5477	1
$\phi_{v,2,10}$	0.06	0	0.05	0.06	0	0	9929	6129	1
$\phi_{v,2,11}$	0.06	0	0.06	0.07	0	0	10538	6178	1
$\phi_{v,2,12}$	0.06	0	0.05	0.06	0	0	9896	5574	1
$\phi_{v,3,1}$	0.04	0	0.04	0.04	0	0	11414	6439	1
$\phi_{v,3,2}$	0.03	0	0.03	0.04	0	0	9798	5627	1
$\phi_{v,3,3}$	0.03	0	0.03	0.04	0	0	10734	5987	1
$\phi_{v,3,4}$	0.05	0	0.04	0.05	0	0	10673	5926	1
$\phi_{v,3,5}$	0.05	0	0.04	0.05	0	0	9349	5958	1
$\phi_{v,3,6}$	0.06	0	0.05	0.06	0	0	10754	5783	1
$\phi_{v,3,7}$	0.06	0	0.06	0.07	0	0	10272	4657	1
$\phi_{v,3,8}$	0.06	0	0.05	0.06	0	0	10641	6067	1
$\phi_{v,3,9}$	0.04	0	0.04	0.04	0	0	10309	5975	1
$\phi_{v,3,10}$	0.03	0	0.03	0.04	0	0	10744	6034	1
$\phi_{v,3,11}$	0.03	0	0.03	0.03	0	0	9690	5983	1

$\phi_{v,3,12}$	0.04	0	0.04	0.05	0	0	11120	5698	1
$\phi_{v,4,1}$	0.07	0	0.06	0.07	0	0	9652	5907	1
$\phi_{v,4,2}$	0.06	0	0.05	0.06	0	0	10980	6462	1
$\phi_{v,4,3}$	0.06	0	0.06	0.07	0	0	11349	6216	1
$\phi_{v,4,4}$	0.07	0	0.07	0.08	0	0	10739	6220	1
$\phi_{v,4,5}$	0.07	0	0.07	0.08	0	0	10310	5831	1
$\phi_{v,4,6}$	0.09	0	0.08	0.09	0	0	10246	6416	1
$\phi_{v,4,7}$	0.1	0	0.09	0.1	0	0	10728	6754	1
$\phi_{v,4,8}$	0.09	0	0.08	0.09	0	0	9592	5772	1
$\phi_{v,4,9}$	0.06	0	0.05	0.06	0	0	11622	6446	1
$\phi_{v,4,10}$	0.05	0	0.05	0.06	0	0	11207	6443	1
$\phi_{v,4,11}$	0.06	0	0.06	0.07	0	0	10755	6102	1
$\phi_{v,4,12}$	0.06	0	0.06	0.07	0	0	10505	6285	1
$\phi_{u,1,1}$	0.02	0	0.02	0.02	0	0	10922	5894	1
$\phi_{u,1,2}$	0.03	0	0.02	0.03	0	0	11361	5584	1
$\phi_{u,1,3}$	0.02	0	0.02	0.03	0	0	11427	6352	1
$\phi_{u,1,4}$	0.03	0	0.02	0.03	0	0	11376	6210	1
$\phi_{u,1,5}$	0.03	0	0.03	0.04	0	0	10965	6786	1
$\phi_{u,1,6}$	0.04	0	0.03	0.04	0	0	11147	5889	1
$\phi_{u,1,7}$	0.04	0	0.03	0.04	0	0	11198	6564	1
$\phi_{u,1,8}$	0.03	0	0.03	0.04	0	0	10219	6359	1
$\phi_{u,1,9}$	0.03	0	0.03	0.04	0	0	10272	5848	1
$\phi_{u,1,10}$	0.02	0	0.02	0.03	0	0	10862	5240	1
$\phi_{u,1,11}$	0.03	0	0.02	0.03	0	0	10723	6120	1
$\phi_{u,1,12}$	0.02	0	0.02	0.03	0	0	10705	5603	1
$\phi_{u,2,1}$	0.03	0	0.02	0.04	0	0	11406	6247	1
$\phi_{u,2,2}$	0.03	0	0.02	0.03	0	0	10643	5851	1
$\phi_{u,2,3}$	0.03	0	0.03	0.04	0	0	10270	6137	1
$\phi_{u,2,4}$	0.04	0	0.03	0.04	0	0	10458	5709	1
$\phi_{u,2,5}$	0.03	0	0.02	0.04	0	0	11914	6146	1
$\phi_{u,2,6}$	0.03	0	0.03	0.04	0	0	10698	6240	1
$\phi_{u,2,7}$	0.04	0	0.04	0.05	0	0	11308	5671	1
$\phi_{u,2,8}$	0.04	0	0.03	0.05	0	0	11501	6088	1
$\phi_{u,2,9}$	0.04	0	0.04	0.05	0	0	12251	6522	1
$\phi_{u,2,10}$	0.03	0	0.03	0.04	0	0	10990	5889	1
$\phi_{u,2,11}$	0.03	0	0.02	0.03	0	0	11299	6116	1
$\phi_{u,2,12}$	0.03	0	0.02	0.03	0	0	11316	6256	1
$\phi_{u,3,1}$	0.02	0	0.02	0.03	0	0	10612	5603	1
$\phi_{u,3,2}$	0.02	0	0.02	0.02	0	0	10629	5784	1
$\phi_{u,3,3}$	0.02	0	0.02	0.02	0	0	10350	5900	1
$\phi_{u,3,4}$	0.03	0	0.02	0.03	0	0	11110	6203	1
$\phi_{u,3,5}$	0.03	0	0.03	0.03	0	0	10779	6195	1
$\phi_{u,3,6}$	0.03	0	0.02	0.03	0	0	10424	5639	1
$\phi_{u,3,7}$	0.03	0	0.03	0.04	0	0	11023	6261	1
$\phi_{u,3,8}$	0.03	0	0.03	0.03	0	0	10894	6681	1
$\phi_{u,3,9}$	0.02	0	0.02	0.03	0	0	9898	6607	1
$\phi_{u,3,10}$	0.02	0	0.02	0.02	0	0	11017	5809	1
$\phi_{u,3,11}$	0.02	0	0.02	0.02	0	0	11048	6114	1
$\phi_{u,3,12}$	0.03	0	0.02	0.03	0	0	11079	6540	1

$\phi_{u,4,1}$	0.03	0	0.03	0.03	0	0	9902	5825	1
$\phi_{u,4,2}$	0.03	0	0.03	0.04	0	0	9889	6374	1
$\phi_{u,4,3}$	0.04	0	0.03	0.04	0	0	11619	6060	1
$\phi_{u,4,4}$	0.04	0	0.03	0.04	0	0	11167	6325	1
$\phi_{u,4,5}$	0.04	0	0.03	0.04	0	0	10676	5979	1
$\phi_{u,4,6}$	0.04	0	0.03	0.04	0	0	10994	5940	1
$\phi_{u,4,7}$	0.04	0	0.03	0.04	0	0	11862	6116	1
$\phi_{u,4,8}$	0.04	0	0.04	0.05	0	0	10466	5658	1
$\phi_{u,4,9}$	0.03	0	0.03	0.04	0	0	11693	6000	1
$\phi_{u,4,10}$	0.03	0	0.02	0.03	0	0	11520	6481	1
$\phi_{u,4,11}$	0.04	0	0.03	0.04	0	0	11332	5724	1
$\phi_{u,4,12}$	0.04	0	0.03	0.04	0	0	12189	7135	1

Beta - Model Comparison

	mean	sd	hdi_3%	hdi_97%	mcse_mean	mcse_sd	ess_bulk	ess_tail	r_hat
τ_1	0.77	0.26	0.31	1.27	0	0	11001	5983	1
τ_2	1.78	0.8	0.45	3.28	0.01	0.01	9672	5975	1
$\Phi_{\alpha,1}$	0.84	0.2	0.46	1.21	0	0	10062	6587	1
$\Phi_{\alpha,2}$	0.93	0.22	0.56	1.38	0	0	10378	6069	1
$\Phi_{\alpha,3}$	0.74	0.18	0.41	1.06	0	0	11336	6069	1
$\Phi_{\alpha,4}$	0.96	0.24	0.55	1.41	0	0	9793	6231	1
$\Phi_{\beta,1}$	0.03	0.01	0.01	0.05	0	0	9968	5615	1
$\Phi_{\beta,2}$	0.04	0.01	0.02	0.06	0	0	9471	6173	1
$\Phi_{\beta,3}$	0.04	0.01	0.02	0.06	0	0	10458	5888	1
$\Phi_{\beta,4}$	0.05	0.02	0.02	0.08	0	0	9258	5397	1
$\phi_{v,1,1}$	4.04	0.55	3.04	5.1	0	0	10169	6061	1
$\phi_{v,1,2}$	2.49	0.33	1.88	3.12	0	0	10226	5996	1
$\phi_{v,1,3}$	4.18	0.57	3.12	5.24	0.01	0	9129	6320	1
$\phi_{v,1,4}$	3.96	0.55	2.97	4.99	0.01	0	9281	6496	1
$\phi_{v,1,5}$	4.5	0.63	3.33	5.65	0.01	0	10650	5455	1
$\phi_{v,1,6}$	4.14	0.57	3.06	5.17	0.01	0	9596	5982	1
$\phi_{v,1,7}$	5.64	0.78	4.17	7.1	0.01	0	11094	5858	1
$\phi_{v,1,8}$	6.87	0.96	5.07	8.67	0.01	0.01	11117	5771	1
$\phi_{v,1,9}$	3.5	0.48	2.62	4.38	0	0	10291	6226	1
$\phi_{v,1,10}$	5.48	0.77	4.07	6.93	0.01	0.01	9448	6409	1
$\phi_{v,1,11}$	3.34	0.46	2.49	4.21	0	0	9637	6113	1
$\phi_{v,1,12}$	3.35	0.46	2.5	4.21	0	0	9734	6080	1
$\phi_{v,2,1}$	3.08	0.48	2.17	3.95	0	0	8998	6245	1
$\phi_{v,2,2}$	3	0.47	2.17	3.89	0	0	10376	6380	1
$\phi_{v,2,3}$	3.68	0.57	2.67	4.78	0.01	0	10170	6303	1
$\phi_{v,2,4}$	4.67	0.75	3.31	6.06	0.01	0	10556	5885	1
$\phi_{v,2,5}$	6.69	1.06	4.83	8.8	0.01	0.01	9743	5878	1
$\phi_{v,2,6}$	6.97	1.12	5.02	9.17	0.01	0.01	10010	6124	1
$\phi_{v,2,7}$	5.38	0.86	3.83	7.05	0.01	0.01	12053	6041	1
$\phi_{v,2,8}$	4.91	0.79	3.5	6.41	0.01	0	12225	6523	1
$\phi_{v,2,9}$	3.54	0.56	2.53	4.58	0	0	10125	6391	1
$\phi_{v,2,10}$	2.96	0.46	2.13	3.81	0	0	10174	5864	1
$\phi_{v,2,11}$	4.74	0.74	3.35	6.07	0.01	0	12225	6132	1
$\phi_{v,2,12}$	4.3	0.68	3.05	5.56	0.01	0	8497	6050	1
$\phi_{v,3,1}$	1.68	0.17	1.37	1.99	0	0	10387	6262	1
$\phi_{v,3,2}$	2.32	0.24	1.9	2.77	0	0	10702	5983	1
$\phi_{v,3,3}$	2.14	0.22	1.73	2.55	0	0	8884	6198	1
$\phi_{v,3,4}$	1.6	0.16	1.31	1.91	0	0	10205	5852	1
$\phi_{v,3,5}$	2.65	0.27	2.15	3.15	0	0	9977	6535	1
$\phi_{v,3,6}$	4.28	0.44	3.47	5.12	0	0	11908	6217	1
$\phi_{v,3,7}$	3.53	0.38	2.84	4.25	0	0	11400	6054	1
$\phi_{v,3,8}$	3.75	0.38	3.05	4.49	0	0	10406	6033	1
$\phi_{v,3,9}$	1.93	0.19	1.59	2.31	0	0	11554	6044	1
$\phi_{v,3,10}$	2.2	0.22	1.78	2.62	0	0	8877	6082	1
$\phi_{v,3,11}$	2.08	0.21	1.7	2.48	0	0	9576	6235	1

$\phi_{v,3,12}$	1.67	0.17	1.36	1.99	0	0	12241	6344	1
$\phi_{v,4,1}$	4.58	0.52	3.62	5.54	0	0	9278	6163	1
$\phi_{v,4,2}$	2.87	0.31	2.27	3.44	0	0	12089	5988	1
$\phi_{v,4,3}$	2.8	0.31	2.23	3.38	0	0	10961	5840	1
$\phi_{v,4,4}$	4.12	0.47	3.2	4.97	0	0	10340	6068	1
$\phi_{v,4,5}$	4.17	0.47	3.34	5.1	0	0	11365	5667	1
$\phi_{v,4,6}$	4.92	0.54	3.93	5.98	0	0	10687	6025	1
$\phi_{v,4,7}$	5.7	0.66	4.55	7	0.01	0	8552	5987	1
$\phi_{v,4,8}$	3.56	0.4	2.85	4.32	0	0	10371	6068	1
$\phi_{v,4,9}$	2.85	0.31	2.28	3.44	0	0	9830	5718	1
$\phi_{v,4,10}$	3.07	0.34	2.44	3.71	0	0	8997	6321	1
$\phi_{v,4,11}$	2.73	0.3	2.16	3.28	0	0	12069	5892	1
$\phi_{v,4,12}$	3.2	0.35	2.54	3.86	0	0	10444	6181	1
$\phi_{u,1,1}$	69.34	10.15	51	88.56	0.1	0.07	9964	6105	1
$\phi_{u,1,2}$	42.21	6.22	31.17	54.31	0.06	0.04	10199	5821	1
$\phi_{u,1,3}$	63.49	9.25	45.25	79.81	0.1	0.07	9088	6601	1
$\phi_{u,1,4}$	54.54	7.97	39.94	69.52	0.08	0.06	9049	6127	1
$\phi_{u,1,5}$	49.34	7.26	36.05	62.99	0.07	0.05	10671	5052	1
$\phi_{u,1,6}$	36.43	5.31	26.34	46.03	0.05	0.04	9579	6475	1
$\phi_{u,1,7}$	44.36	6.4	32.02	56.03	0.06	0.04	11144	5482	1
$\phi_{u,1,8}$	60.01	8.71	44.22	76.62	0.08	0.06	11163	5770	1
$\phi_{u,1,9}$	43.42	6.34	31.55	54.95	0.06	0.04	10274	6099	1
$\phi_{u,1,10}$	75.75	11.18	56.14	97.69	0.11	0.08	9616	6403	1
$\phi_{u,1,11}$	45.78	6.78	33.12	58.37	0.07	0.05	9810	5722	1
$\phi_{u,1,12}$	55.44	8.16	40.76	71.08	0.08	0.06	10055	6362	1
$\phi_{u,2,1}$	41.37	6.95	28.88	54.72	0.07	0.05	9373	6298	1
$\phi_{u,2,2}$	44.72	7.58	31.15	59.49	0.07	0.05	10676	5874	1
$\phi_{u,2,3}$	44	7.28	30.8	57.8	0.07	0.05	9867	6637	1
$\phi_{u,2,4}$	45.43	7.62	31.6	59.64	0.07	0.05	10818	5540	1
$\phi_{u,2,5}$	60.2	9.91	42.4	78.84	0.1	0.07	10023	6456	1
$\phi_{u,2,6}$	58.19	9.62	41.25	76.98	0.1	0.07	10142	6253	1
$\phi_{u,2,7}$	38.6	6.38	26.99	50.95	0.06	0.04	12490	6227	1
$\phi_{u,2,8}$	38.1	6.39	26.67	50.2	0.06	0.04	12125	6195	1
$\phi_{u,2,9}$	31.78	5.32	21.85	41.3	0.05	0.04	10393	6004	1
$\phi_{u,2,10}$	36.47	6.11	25.91	48.87	0.06	0.04	10463	5864	1
$\phi_{u,2,11}$	53.66	8.81	38.24	70.91	0.08	0.06	12026	6181	1
$\phi_{u,2,12}$	54.71	9.1	37.91	71.41	0.1	0.07	8404	6396	1
$\phi_{u,3,1}$	30.48	3.48	24.29	37.15	0.03	0.02	11025	6238	1
$\phi_{u,3,2}$	47.36	5.33	37.18	57.16	0.05	0.04	10804	6085	1
$\phi_{u,3,3}$	46.91	5.35	36.69	57	0.06	0.04	8392	5925	1
$\phi_{u,3,4}$	24.39	2.8	19.23	29.72	0.03	0.02	10446	6256	1
$\phi_{u,3,5}$	39.2	4.38	31.82	48.02	0.04	0.03	10266	6602	1
$\phi_{u,3,6}$	52.63	5.71	42.4	63.68	0.05	0.04	11802	6219	1
$\phi_{u,3,7}$	38.03	4.33	29.99	46.12	0.04	0.03	10909	5551	1
$\phi_{u,3,8}$	46.19	5.01	36.82	55.75	0.05	0.03	10923	6436	1
$\phi_{u,3,9}$	34.7	3.96	27.05	41.96	0.04	0.03	11620	6106	1
$\phi_{u,3,10}$	45.15	5.14	35.52	54.68	0.06	0.04	8695	6196	1
$\phi_{u,3,11}$	48.68	5.51	38.25	58.76	0.05	0.04	10270	6324	1
$\phi_{u,3,12}$	28.18	3.25	22.11	34.46	0.03	0.02	11709	6338	1

$\phi_{u,4,1}$	48.31	5.69	38.1	59.24	0.06	0.04	8638	6506	1
$\phi_{u,4,2}$	34.11	4.05	26.9	42.01	0.04	0.03	12160	6411	1
$\phi_{u,4,3}$	28.96	3.47	22.55	35.5	0.03	0.02	11474	6027	1
$\phi_{u,4,4}$	40.1	4.83	30.75	48.84	0.05	0.03	10423	6325	1
$\phi_{u,4,5}$	40.42	4.81	31.2	49.18	0.04	0.03	11603	5945	1
$\phi_{u,4,6}$	40.33	4.67	31.48	48.98	0.04	0.03	11093	6074	1
$\phi_{u,4,7}$	42.58	5.07	32.99	52.03	0.05	0.04	8666	5310	1
$\phi_{u,4,8}$	28.22	3.31	21.8	34.18	0.03	0.02	10575	5870	1
$\phi_{u,4,9}$	33.98	4	26.36	41.41	0.04	0.03	9934	5623	1
$\phi_{u,4,10}$	39.41	4.74	30.39	47.99	0.05	0.04	8835	5952	1
$\phi_{u,4,11}$	28.4	3.36	22.3	34.85	0.03	0.02	11955	5848	1
$\phi_{u,4,12}$	34.41	4.08	26.9	41.92	0.04	0.03	10080	5906	1

Inverse Gamma - Model Comparison

	mean	sd	hdi_3%	hdi_97%	mcse_mean	mcse_sd	ess_bulk	ess_tail	r_hat
τ_1	2.01	0.73	0.76	3.35	0.01	0	8424	5672	1
τ_2	3.86	1.55	1.25	6.8	0.02	0.01	9409	5791	1
$\Phi_{\alpha,1}$	0.66	0.15	0.38	0.94	0	0	11319	6629	1
$\Phi_{\alpha,2}$	0.71	0.16	0.41	1.01	0	0	10137	6416	1
$\Phi_{\alpha,3}$	0.22	0.05	0.14	0.31	0	0	14658	6109	1
$\Phi_{\alpha,4}$	0.74	0.17	0.43	1.06	0	0	11660	6620	1
$\Phi_{\beta,1}$	0.36	0.11	0.17	0.58	0	0	10709	6937	1
$\Phi_{\beta,2}$	0.34	0.11	0.16	0.55	0	0	9721	6682	1
$\Phi_{\beta,3}$	0.28	0.12	0.09	0.5	0	0	12410	5956	1
$\Phi_{\beta,4}$	0.39	0.12	0.18	0.62	0	0	10938	5411	1
$\phi_{v,1,1}$	3.33	0.45	2.49	4.18	0	0	10350	5476	1
$\phi_{v,1,2}$	2.16	0.29	1.63	2.71	0	0	10599	6426	1
$\phi_{v,1,3}$	3.92	0.53	2.96	4.93	0.01	0	8723	6129	1
$\phi_{v,1,4}$	3.35	0.46	2.52	4.21	0	0	10647	6054	1
$\phi_{v,1,5}$	4.22	0.57	3.21	5.3	0.01	0	9247	6152	1
$\phi_{v,1,6}$	3.58	0.49	2.67	4.5	0	0	9389	6178	1
$\phi_{v,1,7}$	5.38	0.75	4.12	6.94	0.01	0.01	8964	6406	1
$\phi_{v,1,8}$	5.04	0.7	3.76	6.38	0.01	0	9682	5852	1
$\phi_{v,1,9}$	2.61	0.35	1.97	3.27	0	0	9476	6384	1
$\phi_{v,1,10}$	5	0.7	3.66	6.29	0.01	0	9292	6296	1
$\phi_{v,1,11}$	1.24	0.16	0.95	1.54	0	0	10638	5994	1
$\phi_{v,1,12}$	3.4	0.46	2.53	4.25	0	0	9661	6616	1
$\phi_{v,2,1}$	1.66	0.25	1.22	2.15	0	0	9593	6185	1
$\phi_{v,2,2}$	2.51	0.39	1.81	3.25	0	0	9524	5987	1
$\phi_{v,2,3}$	2.46	0.38	1.77	3.2	0	0	9805	6102	1
$\phi_{v,2,4}$	4.59	0.75	3.26	6.03	0.01	0	9598	6105	1
$\phi_{v,2,5}$	7.08	1.15	4.97	9.23	0.01	0.01	11226	5640	1
$\phi_{v,2,6}$	6.32	1.03	4.39	8.22	0.01	0.01	8066	5995	1
$\phi_{v,2,7}$	4.2	0.67	2.99	5.47	0.01	0	10068	6303	1
$\phi_{v,2,8}$	4.66	0.74	3.28	6.05	0.01	0	10854	6148	1
$\phi_{v,2,9}$	2.96	0.47	2.12	3.88	0	0	10560	5844	1
$\phi_{v,2,10}$	3	0.46	2.17	3.9	0	0	12162	6496	1
$\phi_{v,2,11}$	5.12	0.82	3.69	6.74	0.01	0.01	10147	5222	1
$\phi_{v,2,12}$	4.23	0.67	3.03	5.51	0.01	0	11281	6172	1
$\phi_{v,3,1}$	0.08	0.01	0.07	0.09	0	0	17370	5980	1
$\phi_{v,3,2}$	1.94	0.2	1.57	2.29	0	0	11209	6255	1
$\phi_{v,3,3}$	1.36	0.13	1.12	1.61	0	0	9779	6413	1
$\phi_{v,3,4}$	0.08	0.01	0.06	0.09	0	0	16617	5739	1
$\phi_{v,3,5}$	2.31	0.24	1.86	2.74	0	0	11023	5921	1
$\phi_{v,3,6}$	4.37	0.46	3.53	5.25	0	0	10070	5909	1
$\phi_{v,3,7}$	3.66	0.38	2.94	4.37	0	0	9877	5728	1
$\phi_{v,3,8}$	3.49	0.37	2.8	4.17	0	0	9145	6360	1
$\phi_{v,3,9}$	0.08	0.01	0.07	0.1	0	0	17557	5953	1
$\phi_{v,3,10}$	2.26	0.23	1.83	2.7	0	0	11084	6168	1
$\phi_{v,3,11}$	1.24	0.12	1.02	1.46	0	0	10352	5552	1

$\phi_{v,3,12}$	0.08	0.01	0.07	0.09	0	0	17299	5442	1
$\phi_{v,4,1}$	5.36	0.61	4.26	6.51	0.01	0	10213	6115	1
$\phi_{v,4,2}$	2.49	0.28	2.01	3.03	0	0	11223	6337	1
$\phi_{v,4,3}$	2.92	0.32	2.31	3.51	0	0	10062	5889	1
$\phi_{v,4,4}$	3.47	0.39	2.72	4.18	0	0	9586	5828	1
$\phi_{v,4,5}$	3.93	0.45	3.08	4.79	0	0	10430	5150	1
$\phi_{v,4,6}$	4.93	0.56	3.9	5.96	0	0	10902	5950	1
$\phi_{v,4,7}$	5.92	0.68	4.74	7.26	0.01	0	9788	6239	1
$\phi_{v,4,8}$	3.02	0.33	2.4	3.65	0	0	11499	6077	1
$\phi_{v,4,9}$	2.46	0.27	1.98	2.99	0	0	10512	6461	1
$\phi_{v,4,10}$	3.62	0.39	2.88	4.34	0	0	8662	5369	1
$\phi_{v,4,11}$	2.37	0.26	1.86	2.87	0	0	9660	5951	1
$\phi_{v,4,12}$	2.95	0.33	2.35	3.59	0	0	9215	5801	1
$\phi_{u,1,1}$	0.14	0.02	0.1	0.18	0	0	10193	5466	1
$\phi_{u,1,2}$	0.08	0.01	0.06	0.1	0	0	10040	5986	1
$\phi_{u,1,3}$	0.19	0.03	0.14	0.24	0	0	8882	6029	1
$\phi_{u,1,4}$	0.17	0.02	0.12	0.22	0	0	10725	6210	1
$\phi_{u,1,5}$	0.28	0.04	0.21	0.36	0	0	9215	6301	1
$\phi_{u,1,6}$	0.28	0.04	0.21	0.36	0	0	9458	5994	1
$\phi_{u,1,7}$	0.51	0.08	0.37	0.65	0	0	9236	6625	1
$\phi_{u,1,8}$	0.44	0.06	0.32	0.55	0	0	9531	5537	1
$\phi_{u,1,9}$	0.14	0.02	0.1	0.18	0	0	9110	6388	1
$\phi_{u,1,10}$	0.28	0.04	0.2	0.36	0	0	9073	5950	1
$\phi_{u,1,11}$	0.05	0.01	0.03	0.06	0	0	10433	6066	1
$\phi_{u,1,12}$	0.14	0.02	0.1	0.18	0	0	9797	6259	1
$\phi_{u,2,1}$	0.07	0.01	0.05	0.09	0	0	9871	6315	1
$\phi_{u,2,2}$	0.11	0.02	0.07	0.14	0	0	9189	6284	1
$\phi_{u,2,3}$	0.14	0.02	0.09	0.18	0	0	10080	6200	1
$\phi_{u,2,4}$	0.35	0.06	0.24	0.46	0	0	9764	6321	1
$\phi_{u,2,5}$	0.62	0.1	0.43	0.81	0	0	11182	5930	1
$\phi_{u,2,6}$	0.58	0.1	0.41	0.77	0	0	8122	5735	1
$\phi_{u,2,7}$	0.42	0.07	0.29	0.56	0	0	9960	6430	1
$\phi_{u,2,8}$	0.43	0.07	0.3	0.57	0	0	10770	5814	1
$\phi_{u,2,9}$	0.22	0.04	0.15	0.29	0	0	10433	5834	1
$\phi_{u,2,10}$	0.16	0.03	0.11	0.21	0	0	12050	6101	1
$\phi_{u,2,11}$	0.34	0.06	0.24	0.45	0	0	10916	5323	1
$\phi_{u,2,12}$	0.24	0.04	0.17	0.32	0	0	10917	6351	1
$\phi_{u,3,1}$	0	0	0	0	0	0	18033	6000	1
$\phi_{u,3,2}$	0.06	0.01	0.04	0.07	0	0	11350	6086	1
$\phi_{u,3,3}$	0.03	0	0.02	0.04	0	0	9252	6712	1
$\phi_{u,3,4}$	0	0	0	0	0	0	17308	6042	1
$\phi_{u,3,5}$	0.1	0.01	0.08	0.12	0	0	11227	6363	1
$\phi_{u,3,6}$	0.26	0.03	0.21	0.32	0	0	9953	5957	1
$\phi_{u,3,7}$	0.24	0.03	0.19	0.29	0	0	9855	6087	1
$\phi_{u,3,8}$	0.2	0.02	0.16	0.24	0	0	9089	6299	1
$\phi_{u,3,9}$	0	0	0	0	0	0	16401	5753	1
$\phi_{u,3,10}$	0.07	0.01	0.05	0.08	0	0	10524	6275	1
$\phi_{u,3,11}$	0.02	0	0.02	0.03	0	0	10465	6066	1
$\phi_{u,3,12}$	0	0	0	0	0	0	18802	5154	1

$\phi_{u,4,1}$	0.38	0.04	0.3	0.47	0	0	10127	5581	1
$\phi_{u,4,2}$	0.13	0.02	0.1	0.16	0	0	11064	5472	1
$\phi_{u,4,3}$	0.18	0.02	0.14	0.22	0	0	10891	5669	1
$\phi_{u,4,4}$	0.25	0.03	0.19	0.31	0	0	9574	5739	1
$\phi_{u,4,5}$	0.29	0.04	0.22	0.36	0	0	10594	5524	1
$\phi_{u,4,6}$	0.44	0.05	0.34	0.53	0	0	10832	6017	1
$\phi_{u,4,7}$	0.59	0.07	0.46	0.73	0	0	9981	6271	1
$\phi_{u,4,8}$	0.25	0.03	0.19	0.31	0	0	11651	6454	1
$\phi_{u,4,9}$	0.13	0.02	0.1	0.16	0	0	10669	6942	1
$\phi_{u,4,10}$	0.19	0.02	0.15	0.24	0	0	8635	5609	1
$\phi_{u,4,11}$	0.14	0.02	0.11	0.17	0	0	9196	5918	1
$\phi_{u,4,12}$	0.18	0.02	0.14	0.22	0	0	9351	6159	1

A3 Probability Density Functions of Estimated Posterior Distributions over Observed Data

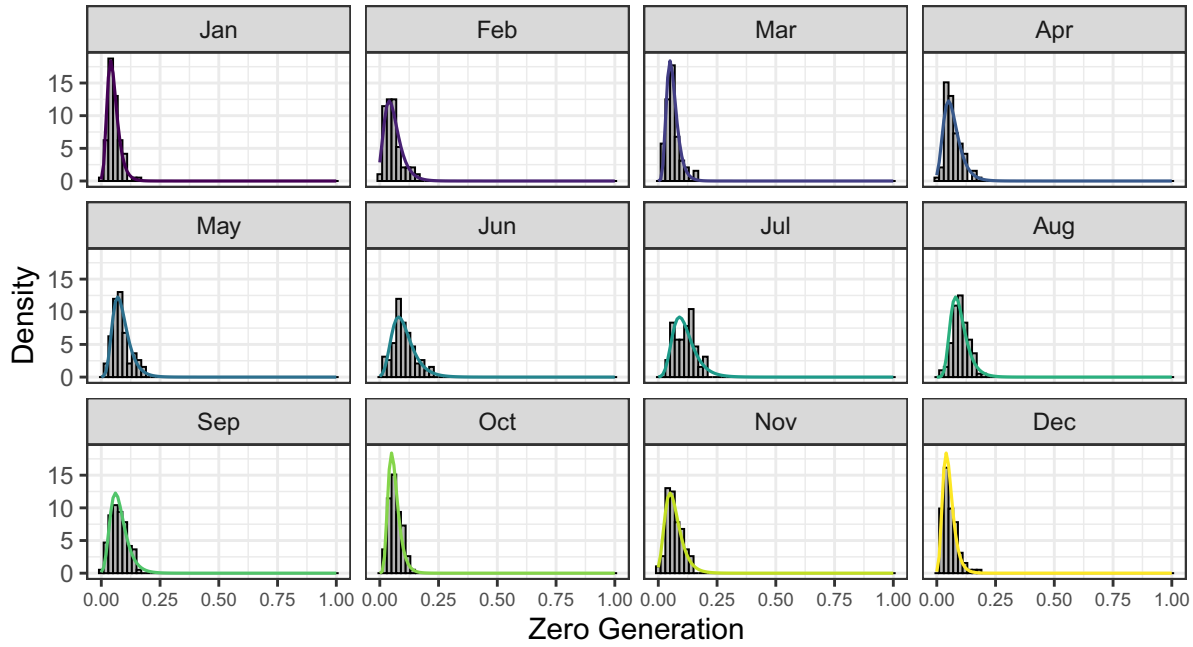

Figure A3.1: Probability Density Functions of estimated posterior probability distributions from the Gumbel-family in the Nordavind-area

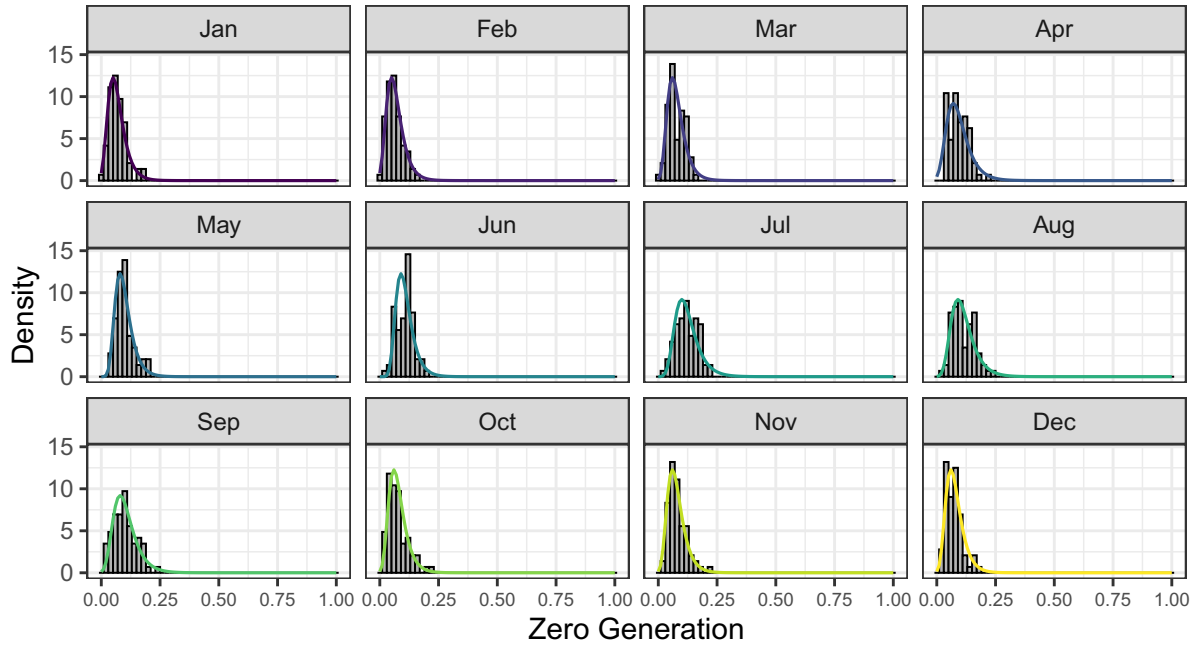

Figure A3.2: Probability Density Functions of estimated posterior probability distributions from the Gumbel-family in the Nordvest-area

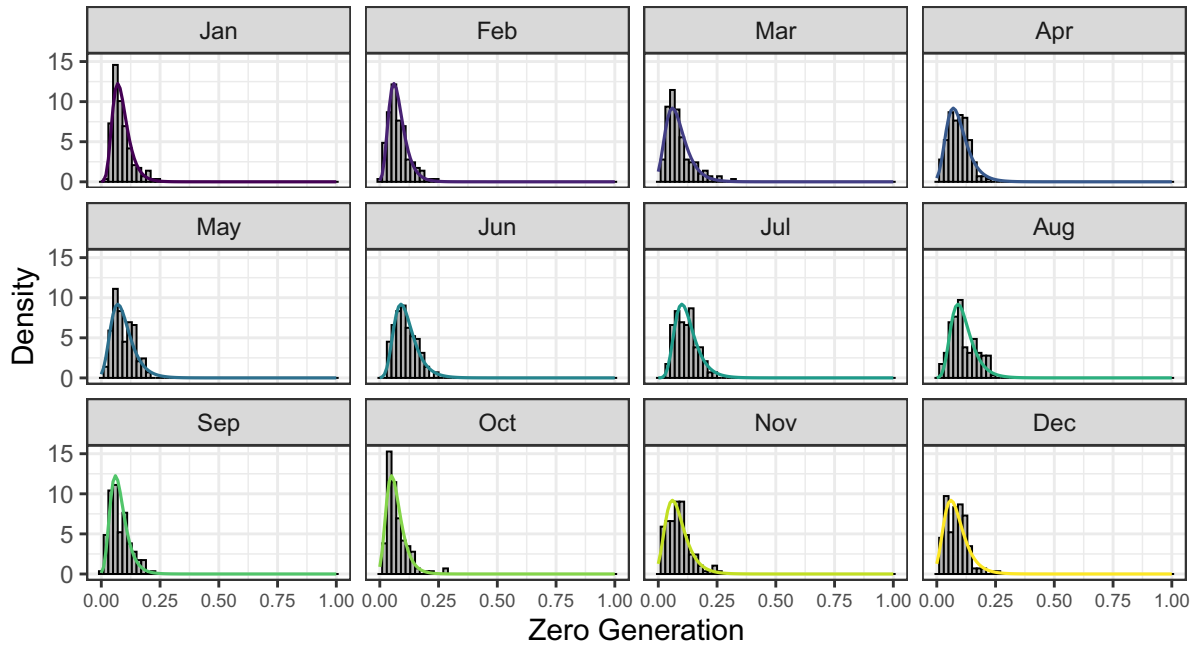

Figure A3.3: Probability Density Functions of estimated posterior probability distributions from the Gumbel-family in the Vestavind-area